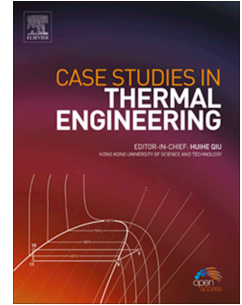


# Journal Pre-proof

Exergy-economic based multi-objective optimization and carbon footprint analysis of solar thermal refrigeration systems

Amin Motevali Emami, Ehsan Baniasadi, Ahmed Rezk



PII: S2214-157X(24)01456-4

DOI: <https://doi.org/10.1016/j.csite.2024.105425>

Reference: CSITE 105425

To appear in: *Case Studies in Thermal Engineering*

Received Date: 14 January 2024

Revised Date: 23 October 2024

Accepted Date: 3 November 2024

Please cite this article as: A.M. Emami, E. Baniasadi, A. Rezk, Exergy-economic based multi-objective optimization and carbon footprint analysis of solar thermal refrigeration systems, *Case Studies in Thermal Engineering*, <https://doi.org/10.1016/j.csite.2024.105425>.

This is a PDF file of an article that has undergone enhancements after acceptance, such as the addition of a cover page and metadata, and formatting for readability, but it is not yet the definitive version of record. This version will undergo additional copyediting, typesetting and review before it is published in its final form, but we are providing this version to give early visibility of the article. Please note that, during the production process, errors may be discovered which could affect the content, and all legal disclaimers that apply to the journal pertain.

© 2024 Published by Elsevier Ltd.

# Exergy-economic based multi-objective optimization and carbon footprint analysis of solar thermal refrigeration systems

Amin Motevali Emami<sup>1</sup>, Ehsan Baniasadi<sup>1,2\*</sup>, Ahmed Rezk<sup>2</sup>

<sup>1</sup>University of Isfahan, Department of Mechanical Engineering, Faculty of Engineering, Hezar-Jerib Ave., Isfahan, Iran, Postal Code 81746-73441

<sup>2</sup>Mechanical, Biomedical and Design Engineering Department (MBDE), College of Engineering and Physical Science, Aston University, Birmingham, B4 7ET, United Kingdom

\* Corresponding author E-Mail: [e.baniasadi@eng.ui.ac.ir](mailto:e.baniasadi@eng.ui.ac.ir); [e.baniasadi@aston.ac.uk](mailto:e.baniasadi@aston.ac.uk)

## Abstract

The increasing carbon footprint associated with conventional cooling methods underscores the urgent need for sustainable alternatives. This study investigates the economic and environmental advantages of various solar-thermal cooling systems, with a focus on optimizing their performance across different climate conditions. Employing a multi-objective approach, the research emphasizes exergy-economic indices to optimize selected cycles. The analysis covers multiple refrigeration technologies, including liquid absorption, solid adsorption, and solid desiccant cycles. Results indicate that the liquid absorption cycle performs optimally in hot, arid climates, reducing the payback period to approximately 8 years when optimized. In hot and humid regions, the solid desiccant cycle proves most effective due to its superior humidity control, yielding a payback period of 5.3 years. For cold and mountainous areas, the solid adsorption cycle is preferred, with a payback period of 13.5 years, while moderate and humid climates benefit from the solid desiccant cycle for both cooling and humidity regulation. The exergy-economic factors for the solar refrigeration systems across semi-arid, hot and arid, hot and humid, cold and mountainous, and moderate and humid climates are 0.758, 0.602, 0.698, 0.74, and 0.575, respectively.

**Keywords:** Solar thermal energy, Liquid absorption, Solid adsorption, Solid desiccant, Optimization, Genetic algorithm, Carbon footprint.

## 1. Introduction

Heavy reliance on fossil fuels raises pressing environmental and energy sustainability challenges. Greenhouse gas emissions from fossil fuel use are a major concern. Buildings account for 40% of total energy consumption and 33% of global greenhouse gas emissions, with heating and cooling alone consuming 40% to 80% of their energy [1]. Increased demand for cooling, especially for air conditioning, due to climate change has prompted a surge in energy consumption. To address this while focusing on clean and sustainable energy, solar cooling systems have gained attention. These systems operate through solar thermal collectors or photovoltaic panels that operate sorption and/or compression refrigeration systems.

Several studies have investigated the utilization of solar-driven cooling systems. Asadi et al. analysed a single-effect water/ammonia solar absorption refrigeration cycle with a 10-kilowatt capacity, which reported that elevating the heat source outlet temperature can enhance both the cycle's energy efficiency and exergy efficiency when various types of solar collectors are used. However, increasing the absorber and condenser temperatures significantly reduced these systems' exergy efficiency [2]. Rompedakis et al. studied solid zeolite-water absorption cycles using a 40 m<sup>2</sup> collector from an environmental perspective. They compared the environmental impact of these systems to conventional refrigeration systems worldwide, demonstrating favourable results

1 regarding the environmental sustainability and feasibility of solar cycles despite their lower  
2 efficiency [3]. Areeba Rahman et al. designed and simulated an absorption solar air-conditioning  
3 system [4]. They optimized it for maximum efficiency and simulated it using TRNSYS software.  
4 The system is simulated for Lahore, Pakistan's climate conditions, and it comprises five thermal  
5 loops: a solar loop consisting of an evacuated glass tube solar collector, a second loop has an  
6 absorption chiller, and an auxiliary furnace with hot water stream, the third is the cooling tower  
7 loop, the fourth loop is of chilled water from the chiller and the final thermal loop is for air delivery  
8 of cooling to each room. The maximum temperature has been achieved around 199 °C. The rated  
9 capacity of the furnace is 41.67 kW with a fluid-specific heat value of 4.19 kJ/kg.K, and the outlet  
10 fluid temperature is set at 115 °C. Abbasi et al. analysed desiccant cycles using TRNSYS software,  
11 comparing various structures in a transient state and assessing single-bed and multi-bed cycles'  
12 efficiency in terms of moisture removal and first and second-law thermodynamic efficiencies [5].  
13 Their research identified the Dunckle arrangement as the most efficient for ventilation and Uckan  
14 for air recirculation, demonstrating that single-bed cycles had higher efficiency than multi-bed  
15 cycles. Nasir Al-Ibrahim investigated the parametric analysis of a two-effect solar absorption  
16 refrigeration cycle using water/lithium bromide, establishing a relationship between the collector's  
17 area and power generation capacity [6]. By optimizing the exergy efficiency of the cycle, they  
18 calculated the maximum possible efficiency, which is valuable for estimating chiller sizes with  
19 various capacities and required collectors.

20 Maher Shehadi explored a solar-powered absorption cycle performance by simulating different  
21 component working temperatures [7]. The coefficient of performance (COP) was optimized against  
22 the generator temperature while varying the other temperatures one at a time. The optimum value  
23 for the evaporator temperature was 10 °C, and for the condenser and absorber was 30 °C. The  
24 optimized COP was almost 0.776 with the above selected components' temperatures and for  
25 generator temperatures higher than 70 °C. The simulation for the proposed optimized system was  
26 run for a 250 square meter (m<sup>2</sup>) house located in Indiana, USA, and it was found that 13 solar  
27 collectors, having a 2 m<sup>2</sup> surface area each. Shakiba Sharifi et al. researched optimizing the energy  
28 and exergy efficiencies of the lithium bromide liquid absorption cycle with a genetic algorithm [8].  
29 Coupling the system with evacuated tube solar collectors increased energy efficiency by up to 9%  
30 and exergy efficiency by up to 3% compared to the non-optimized state. Yu Jing optimized a  
31 closed-loop solar-assisted liquid absorption cooling system, emphasizing exergy-economic  
32 considerations [9]. Optimization of cost functions, including exergy cost and relative difference  
33 exergy cost, led to insights suggesting that refrigeration capacity should be based on the maximum  
34 cooling capacity of the cycle rather than the collector area. Miyanaimi et al. analysed the 3E  
35 (energy, exergy, and exergy-economic) of a multi-purpose solar heating and cooling cycle, using  
36 genetic algorithms for optimization. They adjusted cycle parameters, such as collector outlet  
37 temperatures and vapor flow rates, to maximize exergy efficiency while minimizing exergy costs  
38 and environmental exergy impacts [10]. Ershad et al. employed a genetic algorithm to optimize a  
39 liquid absorption refrigeration cycle, focusing on improving its exergy efficiency. The variable  
40 parameters included the heat exchanger efficiency, vapor flow rate, and temperatures of the coolant  
41 and hot fluid [11]. Farvati et al. analysed the energy and exergy of a two-effect solar absorption  
42 refrigeration system. Their optimization increased the energy efficiency by 5.22% and an exergy  
43 efficiency boost of 4.95% [12].

44 Asgari et al. simulated a solar thermal cooling system in Tehran from 2017 to 2020 using  
45 engineering equation solver (EES) software with vacuum tube high efficiency collectors [13]. They

1 accomplished an economical analyse which resulted in 21161 USD for net present value and 10  
2 years payback period. Baiju et al. have modelled a solar two-bed adsorption refrigeration system  
3 with MATLAB software by using Dubinine Astakhov model to simulate the gas adsorption  
4 between activated carbon micro pores beds [14]. They achieved a maximum coefficient of  
5 performance (COP) of 0.68 and the highest exergy efficiency of 5%. Mortadi et al. presented a  
6 numerical model for solar absorption and solar adsorption cooling systems using Energyplus  
7 software for a typical office building to evaluate the performance, economic and environmental  
8 indices [15]. They concluded that the increase in solar fraction impacts the economic and  
9 environmental indicators positively, because the levelized cost of cooling, discounted payback  
10 period and life cycle performance values are reduced. Moreover, solar adsorption cooling system  
11 was found to be the most environmentally friendly since it exhibits the lowest life cycle cost (LCC)  
12 value. Tareq Salameh et al. simulated a solar absorption cooling system based on a LiBr–H<sub>2</sub>O in  
13 UAE for a residential house by TRANSYS software [16]. The proposed system yielded a COP of  
14 0.793. The optimization results showed that the latitude of the UAE is the optimum tilt angle for  
15 the evacuated tube at 0.73 solar fraction (SF). Additionally, the life cycle analysis indicates that the  
16 solar absorption cooling system incurs 43.2% cost, utilizes 8.5% of the energy, and generates a  
17 carbon footprint 8.7% of the combined system. Auroshis Rout et al. conducted a 3E (Energy,  
18 Exergy, Economic) analysis for a novel off-grid solar polygeneration energy technology producing  
19 electricity using photovoltaic panels and hot water along with hot air using a solar thermal system  
20 across four Indian provinces with four different climates [17]. The values of annual average energy  
21 efficiency of the solar thermal system are 64.6% for Andhra Pradesh, 64.5% for Madhya Pradesh,  
22 64.2% for Uttar Pradesh, and 58.3 for Union territory, while exergy efficiency is found to be 1.3%,  
23 1.4%, 1.2%, and 0.7%, respectively. For the solar thermal unit, the values of payback period are  
24 obtained as 5.2, 5.5, 7.5, 9.4 years, respectively. Thomas et al. designed a solar thermal energy-  
25 based hybrid polygeneration system located on an island in the Indian Ocean with end products  
26 such as electricity, heating, cooling for food storage, and desalinating to get pure water [18]. They  
27 found that the annual carbon emissions that are curtailed with solar thermal polygeneration outputs  
28 are cumulated and found to be 434 tonnes of carbon. The social cost and environmental cost due to  
29 carbon mitigation are considered as an incentive in the cost economic economics of polygeneration  
30 system and it is found that the Internal Rate of Return (IRR) and payback can be improved to  
31 17.98% and 6.2 years respectively. Thomas et al. analysed the energy and exergy of a solar thermal  
32 based polygeneration process used for rural application in India by Linear Fresnel reflector (LFR)  
33 [19]. Vapour Absorption Machine (VAM) and adsorption chiller are selected for cooling  
34 applications The system is integrated with a thermal energy storage application most of the  
35 equipment experiences less exergy loss. The LFR and VAM are found to have the most  
36 contribution in irreversibility incurred compared to others components and hence these components  
37 need to be focused.

38 Considering the existing knowledge in the literature, there is an important gap regarding economic  
39 and environmental perspectives that can be identified using exergy-economic and carbon footprint  
40 analyses. The author's previous work undertook a technical and thermodynamic simulation of solar  
41 thermal cooling systems, and this research builds on the previous research on the dynamic  
42 simulation and exergy-economic assessment of solar thermal refrigeration systems in various  
43 climates that have been undertaken to further develop the established modelling for solar-thermal  
44 cooling systems in different climatic zones such as tropical, sub-tropical, moderate, cold, hot and  
45 moist regions [20]. The objective is to conduct a more detailed examination and to enhance the

1 performance of the proposed refrigeration systems. The contribution of this work lies in optimizing  
 2 the performance of former simulated systems based on energy, exergy, and exergy-economic  
 3 parameters, which can elucidate ambiguities around the low coefficient of performance in these  
 4 systems. Conducting such analysis and optimization using a genetic algorithm is rarely found in  
 5 similar research studies.

## 7 **2. Solar radiation atlas for various climates in Iran**

8 Iran is one of the world's sunniest countries, with over 300 sunny days and an average solar  
 9 radiation of 4.5-5.5 kilowatts per square meter daily. It led to emphasizing on solar energy  
 10 utilization in its climate. To better estimate available solar radiation across Iran's extensive  
 11 geographical regions, determining the received radiation levels in each area is essential [20].  
 12 Recently, the Iranian Renewable Energy Organization has published a comprehensive and reliable  
 13 Solar Radiation Atlas, aligning well with data extracted from similar sources such as NASA. This  
 14 atlas divides Iran's climate, in terms of received solar radiation, into four primary regions, each  
 15 possessing substantial potential. Since this research focuses on the application of climate control  
 16 systems, other factors such as weather conditions, relative humidity, and more must be considered  
 17 in climate classification. Therefore, to enhance the accuracy of the atlas, an additional region can be  
 18 added to the previous regions, specifically for the northern Persian Gulf and Oman Sea area. This  
 19 region boasts high solar radiation potential and holds a prominent position in terms of relative  
 20 humidity in Iran's geography. The humidity adjustment, especially during hot seasons in coastal  
 21 regions, is crucial and significantly influences the selection of the most appropriate and efficient  
 22 cooling system.

23 Figure 1 illustrates the modified atlas, and Table 1 presents the solar radiation intensity in each  
 24 geographical area. Furthermore, a representative city has been selected for each climate, and all  
 25 analyses and investigations pertinent to that climate have been conducted on the selected city [20].  
 26 The colours used in Table 1 correspond to the climatic regions outlined in the solar map.

27  
 28 Table 1: Radiative characteristics of different regions in Iran [20]

<b>Solar intensity</b> ( <i>kWh/m<sup>2</sup> day</i> )	<b>Representative</b> <b>City</b>	<b>Climate</b>
2.8-3.8	Ramsar	Moderate and moist climate
3.8-4.5	Tabriz	Cold and arid climate
4.5-5	Isfahan	Semi-arid climate
5 -5.3	Bushehr	Hot and moist climate
5.3-5.6	Kerman	Hot and arid climate

29

30

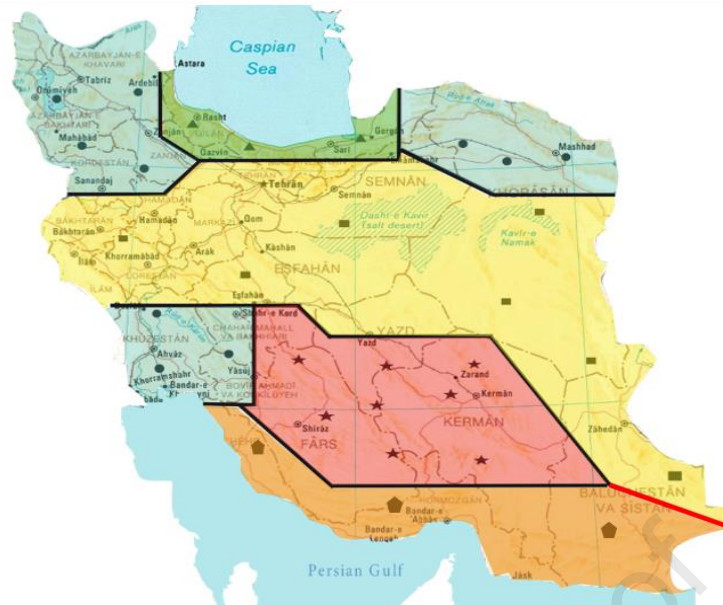


Figure 1: The proposed solar irradiation atlas for Iran's climate [20]

1  
2  
3

### 3. Research methodology

4 By selecting one of the climate zones mentioned above (1), the required meteorological and climate  
5 data for the chosen region is retrieved using Meteonorm software from its online databases (2). The  
6 thermal load of the reference building is calculated using Carrier HAP software, which simulates  
7 the building's performance in the selected climate zone, based on the data extracted from  
8 Meteonorm. This process generates hourly cooling load profiles following the method described by  
9 Duanmu et al. [21] (4). The extracted data such as temperature, humidity, and solar radiation are  
10 compiled into a simulation database (7), along with elementary economic and environmental  
11 parameters, including interest rates, CO<sub>2</sub> factors, and initial investment values (6).

12 Subsequently, different thermodynamic simulations and modelling of the integrated refrigeration  
13 systems, closed-loop liquid absorption, closed-loop solid adsorption, and solid desiccant systems  
14 are performed for the selected climate zone using EES software, based on the compiled database  
15 (8). EES, an engineering equation solver, is coupled with a thermodynamic library to calculate the  
16 properties of the working fluids at each stage of the cooling cycles. The software utilizes the  
17 relevant thermodynamic equations and libraries for each working fluid.

18 These steps analyse the system using the 3E method (Energy, Exergy, and Economics), calculating  
19 key metrics such as solar radiation received by the collectors, energy extracted, auxiliary heater  
20 load, fuel consumption, and exergy balance results (9). The enhanced energy, exergy, and  
21 economic results, along with the primary environmental and economic data in the database, are  
22 further processed in EES to conduct a parametric study, environmental analysis, and exergy-  
23 economic analysis (10). This technical analysis precedes the economic and environmental  
24 assessments of the refrigeration systems, with key parameters such as payback period and carbon  
25 emissions evaluated on an hourly, daily, monthly, and annual basis. Exergy-economic factors are  
26 determined for each cooling system in the selected climate.

27 Furthermore, the optimization of the chosen systems is carried out using a genetic algorithm (GA)  
28 based on exergy-economic indicators and EES software (13). The first step in this optimization  
29 involves selecting target indicators such as exergy-economic factors and irreversibilities to  
30 optimize using the described method (11). Next, the variable parameters and their ranges are  
31

1 defined and input into the software (12). The optimized results are then compared to the initial  
 2 conditions to assess improvements (14). Figure 2 illustrates the methodology flowchart.

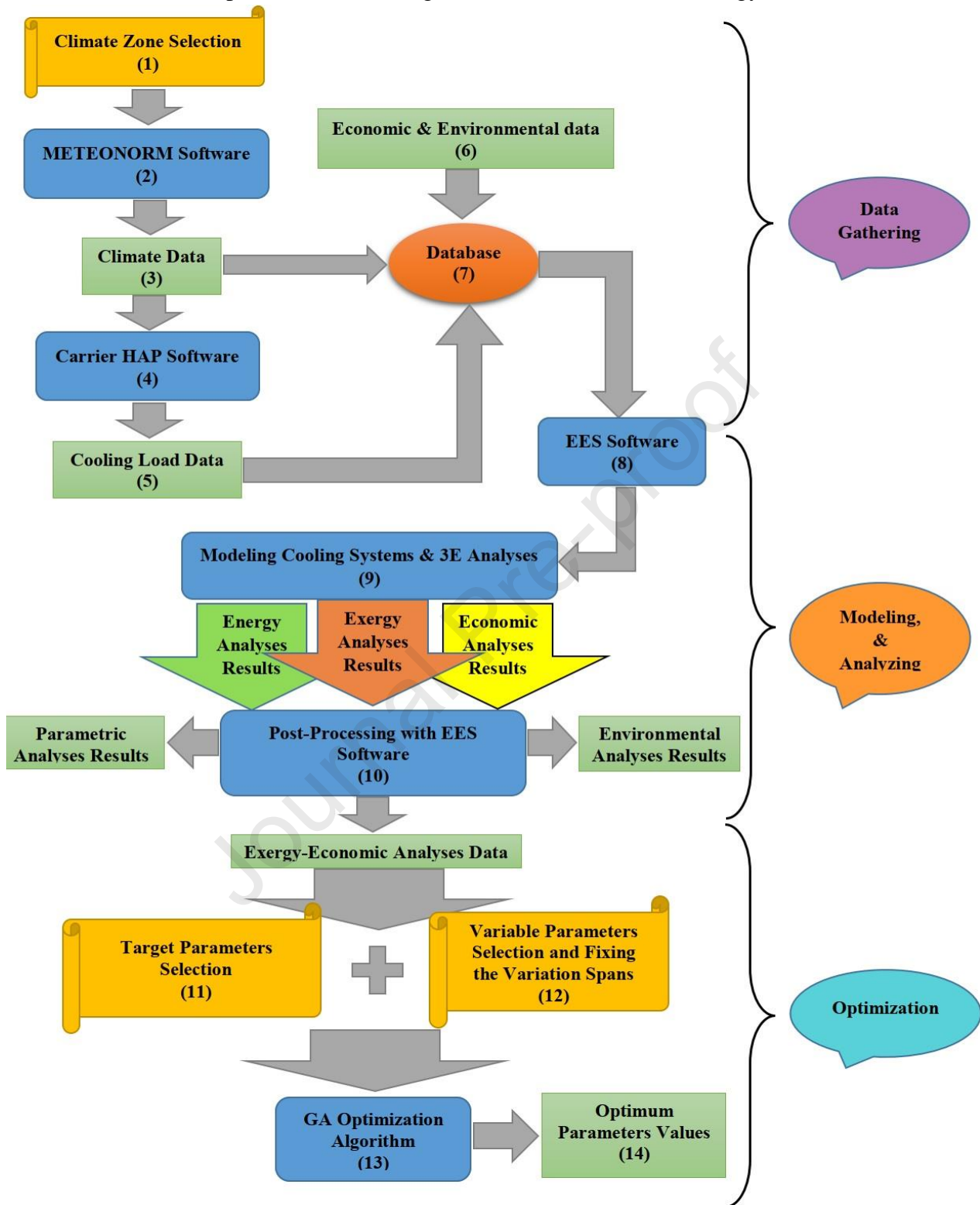


Figure 2: Exergy-economic and optimization flowchart

### 3.1. Fundamental data for each climate and reference building specifications

#### 3.1.1 Hot season declaration

The duration of the hot season varies in each climate of Iran and has its specific timeframe. The consecutive hot days are defined as the hot season for each climate as follows [34]:

- Semi-arid Climate (Isfahan city): from day 140 to day 260 = 120 day a year.

- 1 • Warm and Dry Climate (Kerman city): from day 120 to day 280 = 160 days a year.
- 2 • Warm and Humid Climate (Bushehr city): from day 95 to day 295 = 200 days a year.
- 3 • Cold and Mountainous Climate (Tabriz city): from day 150 to day 260 = 110 days a year.
- 4 • Moderate and Humid Climate (Ramsar city): from day 120 to day 260 = 140 days a year.

### 3.1.2 Specifications of solar collectors

By calculating the available area on the roof of the reference building (assuming the use of 80% of the roof area), installing 25 solar collectors, each with dimensions of 4x2 meters and an absorber area of 6.2 m<sup>2</sup> is feasible. These collectors are arranged in two rows with a spacing of 0.6 meters.

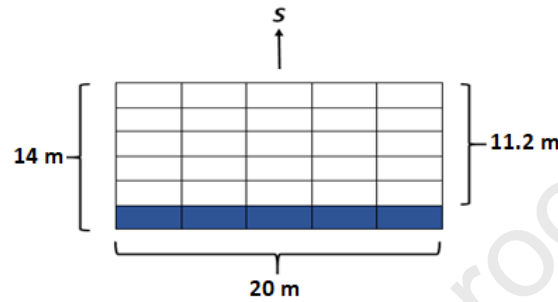


Figure 3: Arrangement of solar collectors on the roof [20]

### 3.1.3 Specifications of reference building

The reference building is characterized as follows:

- 15 • 5-story residential building.
- 16 • Total floor area: 1625 m<sup>2</sup>.
- 17 • Roof area: 20x14 meters (280 m<sup>2</sup>).
- 18 • Floor 1: 180 m<sup>2</sup>.
- 19 • Floors 2 to 4 (2 units per floor): Each unit covers 150 m<sup>2</sup>.
- 20 • Floor 5: 245 m<sup>2</sup>.

## 4. Solar-thermal refrigeration cycle configurations

### 4.1. Solar-thermal driven liquid absorption refrigeration system

As the most commercially available option lithium bromide-water solution is selected as the absorbent and refrigerant in this process. This mixture undergoes absorption in the heat generator, leading to the separation of pure water vapor. After pressure reduction, the high-concentration lithium bromide solution cycles back to the absorber as water vapor. This condensed water vapor enters the evaporator, cooling it as it exchanges heat with the low-temperature refrigerant, raising its temperature. The high-temperature working fluid descends and mixes with the returning flow from the generator, facilitating absorption. Cooling water is provided to remove heat from the main flow, then proceeds to the condenser, transforming the refrigerant from vapor to liquid. The generator is heated by hot water from two heat sources, primarily solar collectors with an auxiliary heater and natural gas for additional temperature boost. The generator simultaneously increases temperature and pressure and evaporates the refrigerant [20].





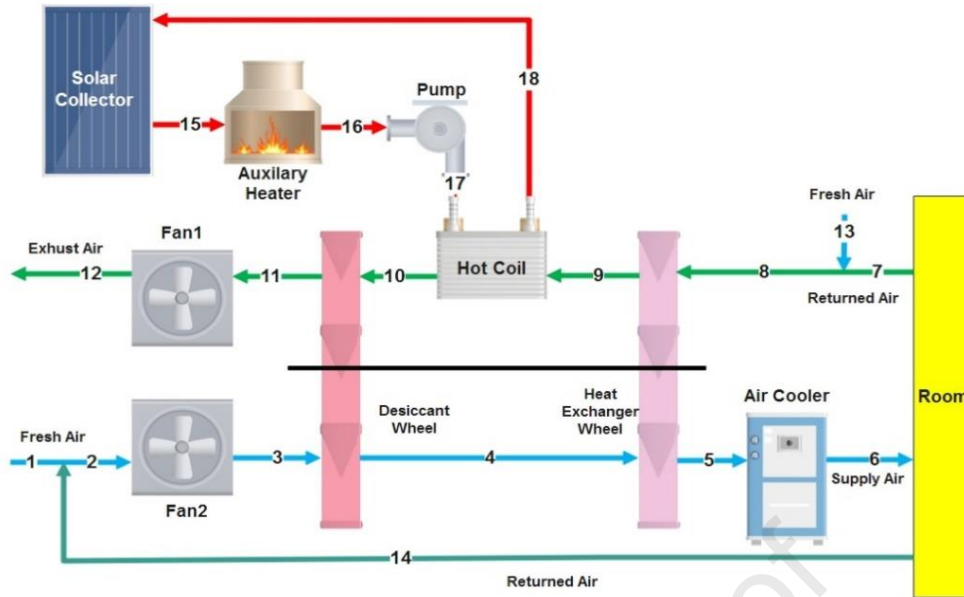


Figure 6: Flow diagram of the solar-thermal solid desiccant cooling cycle [20]

## 5. Governing equations

### 5.1. Incident solar energy

In order to calculate the useful heat received by the hot water flow from the solar collectors, we require several parameters, including slope angle (which is approximately equal to the latitude of the location), the collector efficiency (extracted from the technical specifications of the collector in use), the absorber area, and the total solar irradiation incident on the inclined collector surface. For determination of the total incident solar irradiation on the inclined surface of the collector used the values of direct and diffuse radiations and employing the isotropic sky model [22].

### 5.2. Components Thermodynamic model

By neglecting changes in kinetic and potential energy, the energy balance in each component of the cycle can be written as [23]:

$$\dot{Q} - \dot{W} = \sum \dot{m}_{out} h_{out} - \sum \dot{m}_{in} h_{in} \quad (1)$$

The ideal overall exergy of the flow streams, assuming no alteration in the chemical composition of the working materials, is calculated using equation 2 [23]:

$$\dot{E}X = \dot{m}((h - h_0) - T_0(s - s_0)) \quad (2)$$

By neglecting changes in kinetic and potential energy, the exergy balance can be undertaken utilizing equation 3 [8]:

$$\dot{Q} \left(1 - \frac{T_0}{T}\right) - \dot{W} = \sum \dot{m}_{out} h_{out} - \sum \dot{m}_{in} h_{in} + \dot{I} \quad (3)$$

The exergetic efficiency can be determined using equation 4 [24].

$$\varepsilon = \frac{\text{coolingload} \left(1 - \frac{T_0}{T}\right)}{Q_{collector} \left(1 - \frac{T_0}{T}\right) + Q_{heater} \left(1 - \frac{T_0}{T}\right) + \Sigma W_p + \Sigma W_f} \quad (4)$$

The cycle's coefficient of performance (COP) is defined as total cooling load to total heat gain from solar collectors, auxiliary heater and input electrical energy to pumps, as indicated in equation 5 for assessing the system's energy conversion efficiency.

$$COP = \frac{\dot{Q}_{eva}}{\dot{Q}_{gen} + \dot{W}_p} \quad (5)$$

The performance assessment of a solar cooling system typically involves the utilization of the solar fraction. This metric quantifies the proportion of solar energy input that contributes to the cooling effect concerning the overall input energy demand, encompassing both the main and auxiliary heating systems. One can divide the total input thermal energy to the above mentioned systems to two exact sources: solar and natural gas. In order to assess the solar collector effectiveness and its contribution to reduce the auxiliary heater load during a day or hot season, the solar fraction is defined that describes a relation between total input heat to the cooling system and the solar thermal energy contribution as follows [33]:

$$SF = \frac{Q_{solar}}{Q_{solar} + Q_{Aux}} \quad (6)$$

### 5.3. Exergy-economic study

Exergy-economic analysis bridges thermodynamics and economic indices. The magnitude of exergy dissipation within a system not only signifies the thermodynamic inefficiency of said system but also presents an avenue for potential capital cost reduction. Once the exergy balance has been determined at the component level, the exergy cost associated with each stream can be determined.

$$\dot{C}_{F,k} = c_{F,k} \dot{E}x_{f,k} \quad (7)$$

Where  $\dot{E}x_{f,k}$  denotes the rate of exergy cost for the fuel stream in the equipment, and  $C_{f,k}$  denotes the unit cost of exergy for the fuel stream in each equipment [25].

$$\dot{C}_{Q,k} = c_{Q,k} \dot{E}x_{Q,k} \quad (8)$$

To calculate  $\dot{Z}_k$ , which is the investment cost of each component, the following process should be followed. The number 3600 represents the seconds in an hour, and 8200 represents the annual working hours [25]:

$$\dot{Z}_k = \frac{\Phi_k AC_k}{3600 \cdot 8200} \quad (9)$$

where  $\Phi_k$  denotes the maintenance factor attributed to each component that is defined as follows [26]:

$$\Phi_k = 1.068 AC_k \quad (10)$$

where  $AC_k$  is the annual cost of each component as follows [26]:

$$AC_k = PW_k CRF \quad (11)$$

Where  $CRF$  is the value-added factor that is defined as follows:

$$CRF = \frac{ii(1+ii)^n}{(1+ii)^n - 1} \quad (12)$$

The interest rate is assumed to be 0.25, and the service life is 15 years [26]. The  $PW_k$  parameter represents the current value of the asset, and it is defined as follows [26]:

$$PW_k = C_k - S_{k,n} PWF \quad (13)$$

Where  $S_{k,n}$  represents the salvage value of the asset after 15 years, and it is equal to 10% of the purchase cost of the asset [26]:

$$S_{k,n} = 0.1C_k \quad (14)$$

$C_k$  denotes the initial investment cost or the equipment purchase cost [26]. The exergy-economic factor of the system is equivalent to the ratio of the system's current expenses, excluding exergy destruction costs, to the total current expenses of the system, encompassing exergy destruction costs [27].

$$f_k = \frac{\dot{z}_k}{\dot{z}_k + c_{f,k} \dot{i}_k} \quad (15)$$

The main assumptions assigned to the unit costs of exergy for both thermal and work streams, which include inflows and outflows within the system are listed below [20]:

- The exergy unit cost of fan power ( $c_f$ ): 0.05 [\$/kW].
- The exergy unit cost of pump power ( $c_p$ ): 0.05 [\$/kW].
- The exergy unit cost of transferred heat in the cooling tower ( $c_{ct}$ ): 0.00001 [\$/kW].
- The exergy unit cost of transferred heat in solar collectors ( $c_{collector}$ ): 0.00001 [\$/kW].
- The exergy unit cost of transferred heat in the auxiliary heater ( $c_{ct}$ ): 0.017 [\$/kW].
- The exergy unit cost of transferred heat in cooler ( $c_{cooler}$ ): 0.012 [\$/kW].

#### 5.4. Economic and environmental evaluations

The economic evaluation of solar cooling systems in different climates is based on the definition of two main scenarios. In Scenario 1, simultaneous and combined use of solar energy and fossil fuels to provide thermal energy for cooling cycles. In this scenario, the required hot water in the system is initially directed to the solar collectors installed on the building's rooftop. After receiving a certain amount of heat, it enters the auxiliary heater. After measuring the inlet temperature and calculating the difference to the required temperature for the generator, it receives heat from the auxiliary heater to reach the desired temperature. The heat created in the auxiliary heater is obtained from the energy generated by the combustion of natural gas.

In Scenario 2, continuous and sole utilization of a gas-fired heater system with a greater capacity than in Scenario 1. In this scenario, it is assumed that no solar system is employed, and all the thermal load required by the system is met using a natural gas boiler. The objective of defining these two recent scenarios is to assess and compare the economic and operational performance of the hybrid system. Subsequently, by defining two general methods, the initial capital investment cost, the service life cost, and the simple payback period can be determined, considering the utilization of the hybrid system.

The initial capital investment costs for each piece of equipment in these cycles, including chillers, cooling towers, evacuated tube solar collectors, pumps, fans, and auxiliary boilers, have been factored in, considering factors obtained from domestic and international manufacturers. Maintenance and repair costs, contingent upon usage type, duration of operation, and equipment type used in each cycle, have been averaged between 1% and 1.5% of the total initial capital investment cost per year [30]. The operational costs of the systems, encompassing gas and electricity consumption, have been obtained by calculating electricity and gas consumption values for each cycle through hourly thermodynamic calculations for each day during the warm season. These values are then aggregated to determine annual electricity and gas consumption. The unit cost for each cubic meter of gas consumed has been set at \$12, and the cost for each kilowatt-hour of electricity consumed is around 6 USD cents in 2023.

1 Equations 16-25 are employed for the economic evaluation. Equation 16 determines the parameter  
 2 SPP, in which the discount and interest rates do not interfere, based on the initial capital investment  
 3 cost and the annual operating cost [31].

$$4 \quad SPP = \frac{InitialInvestment}{NetAnnualCashinflow} \quad (16)$$

5 Equation 17 determines the system's present value and provides a more precise method for  
 6 calculating the payback period.

$$7 \quad NPV = \sum_{n=0}^{15} \frac{CashFlow}{(1+ir)^n} - INV \quad (17)$$

8 In this study, the initial investment cost is first calculated annually, taking into account the interest  
 9 rate [31].

$$10 \quad A_{Inv} = Inva \quad (18)$$

11 Using Equations 19 and 20, the discounted rate for each year (over the system's lifespan, T) is  
 12 calculated separately. The discount rate (*ir*) value was 2.5%, and the solar cooling system's lifespan  
 13 is 15 years [31].

$$14 \quad q = 1 + ir \quad (19)$$

$$15 \quad a = \frac{(q-1)q^T}{(q^T-1)} \quad (20)$$

16 Equation 24 is used to calculate the annual current expenses, taking into account the annual interest  
 17 rate for each system. The cost escalation rate (i.e., interest) (*p*) can vary for energy carriers and  
 18 equipment, which was considered 5%, as recommended by xx et al. [31].

$$19 \quad CV_n = CV_1(1 + p)^{n-1} \quad (21)$$

20 The annual discount rate for the total value of annual current expenses is applied using equation 22  
 21 [31]:

$$22 \quad DVP = \sum_{n=1}^T \frac{CV_n}{(1+ir)^n} \quad (22)$$

23 The total current system cost until the end of the desired year is calculated using equation 23 [31]:

$$24 \quad A_{DPV} = DVPa \quad (23)$$

25 The maintenance cost of the system is also considered as part of the current expenses, similar to  
 26 electricity or gas costs, and it is calculated using equation 24 [31]:

$$27 \quad CV_{maintenance} = MaintenanceFactorInv(1 + p)^{n-1} \quad (24)$$

28 Finally, according to equation 25, the system's cumulative life cost until the end of the desired year  
 29 is calculated [31].

$$30 \quad LCC = A_{DPV} + A_{inv} \quad (25)$$

31 Table 2 presents the capital investment cost for each system used in various climates.

1 It should be noted that the calculated capital costs for each refrigeration cooling system are  
 2 obtained by summation of constituent component prices which are inquired from the international  
 3 manufacturers based on relevant cooling load and required heating load in each climate region, plus  
 4 engineering, installation, assembly, freight and commissioning costs.

6 Table 2: Initial capital investment costs for proposed cycles in each climate

Liquid Adsorption	Solid Adsorption	Solid Desiccant	Liquid Adsorption	Solid Adsorption	Solid Desiccant	Liquid Adsorption	Solid Adsorption	Solid Desiccant	Liquid Adsorption	Solid Adsorption	Solid Desiccant	Liquid Adsorption	Solid Adsorption	Solid Desiccant	System	Initial investment [€]
77183	140788	141895	47849	56350	79111	56751	96282	82681	67841	117869	82919	84058	152272	117012		

7 After calculating the natural gas consumption savings during the execution of Scenario 1 by finding  
 8 the difference in gas consumption between the two proposed scenarios on an hourly, daily, and  
 9 annually basis, the reduction in the emission of greenhouse gases such as CO<sub>2</sub>, NO<sub>x</sub>, and CO can  
 10 be calculated for each hour and annually using the relevant emission coefficients [32]. These  
 11 coefficients indicate the amount of the desired gas produced per unit mass or volume of natural gas  
 12 consumed [32]. It is worth mentioning, that the main source of CO<sub>2</sub>, CO and NO<sub>x</sub> emissions in this  
 13 system is the auxiliary heater that is used to achieve the required working fluid temperature after  
 14 using solar collectors.

- Carbon dioxide (CO<sub>2</sub>) emission coefficient: 2.75 kg/kg fuel.
- Carbon monoxide (CO) emission coefficient: 0.0009 kg/kg fuel.
- Nitrogen dioxide (NO<sub>x</sub>) and other emissions coefficient: 0.00185 kg/kg fuel.

### 19 5.5. Optimization procedure

20 The multi-objective optimization was undertaken using the genetic algorithm approach. It is an  
 21 evolutionary algorithm that employs principles from evolutionary biology, such as inheritance and  
 22 biological mutation, to determine the optimal correlations for predicting or pattern matching.  
 23 Genetic algorithms are often a suitable choice for prediction techniques based on regression and  
 24 optimization. The genetic algorithm continuously refines a population of individual solutions. In  
 25 each step, this algorithm randomly selects individuals from the current generation as parents and  
 26 uses them to create offspring, who become members of the next generation. Over successive  
 27 generations, the population of solutions evolves towards an optimal solution. Also genetic  
 28 algorithms offer a viable approach for addressing mixed-integer nonlinear programming problems,  
 29 particularly those where specific variables are constrained to integer values [29].

30 Multiobjective optimization was undertaken considering energy efficiency, exergy efficiency and  
 31 exergy-economic factor as the objectives, incorporating technical and economic indices such as  
 32 solar fraction, primary energy, fuel consumption, pollutant emissions, fuel savings, irreversibility,  
 33 annual operating costs, payback period, exergy-economic factor. Tables 3 to 7 provide the variable  
 34 parameters used in multi-objective optimization for each city alongwith their initial values, optimal  
 35 values, and specified ranges for each parameter. The objective functions are coefficient of  
 36 performance (COP), Exergy efficiency ( $\epsilon$ ), and exergy-economic factor ( $f_k$ ).

37 As it is announced former, all of assumed cooling systems are modeled and simulated by EES software in  
 38 this work and key parameters for these cycles were stated by our researches based on usual existing

1 commercial systems. In each climate zone the best techno-economic efficient system was selected and then  
 2 due to the selected cooling system in every climate region, all of possible variable parameters were selected  
 3 defined according to the simulation conditions. It is tried to emphasis more on solar parameters to evaluate  
 4 the effects of their variation on selected systems performance. In next step, one logical and doctrinaire  
 5 variation span defined for each selected parameters in previous step based on simulation limits.

Table 3: Variable parameters of liquid absorption cycles in Isfahan city

Parameter	$X_1$	Diff Lat & Tilt	$\dot{m}_{19}$	$\dot{m}_{16}$	$\dot{m}_{14}$	$Q_2$	$Q_5$	$P_{10}$	$P_3$	$T_{14}$	$T_{19}$	$T_{17}$
Primary	0.98	-2	4	2	4	0.55	0.6	1	8	20	15	85
Min	0.8	-10	2	1	2	0.2	0.55	1	5	15	5	75
Max	1	10	8	5	8	0.7	1	10	20	25	20	100
Optimized	0.99	-5	2	2.2	4	0.4	0.6	1	6.5	19	15	75

Table 4: Variable parameters of liquid absorption cycles in Kerman city

Parameter	$X_1$	Diff Lat & Tilt	$\dot{m}_{19}$	$\dot{m}_{16}$	$\dot{m}_{14}$	$Q_2$	$Q_5$	$P_0$	$P_3$	$T_{14}$	$T_{19}$	$T_{17}$
Primary	0.97	-2	4	2	4	0.55	0.6	1	8	20	15	85
Min	0.8	-10	2	1	2	0.2	0.55	1	5	15	5	71
Max	1	10	8	5	8	0.7	1	10	20	25	20	101
Optimized	0.99	-6	2	2.2	4	0.4	0.65	2	6.5	18	15	78

Table 5: Variable parameters of solid desiccant cycles in Bushehr city

Parameter	Diff Lat & Tilt	$\dot{m}_{15}$	$T_{16}$	$T_4$	$T_n$	$RH_{in}$
Primary	-2	2	85	56	23	0.5
Min	-10	1	75	45	20	0.3
Max	10	5	100	70	28	0.7
Optimized	-7.5	1	75	65	24	0.45

Table 6: Variable parameters of solid adsorption cycles in Tabriz city

Parameter	$X_5$	Diff Lat & Tilt	$\dot{m}_{14}$	$\dot{m}_{10}$	$\dot{m}_6$	$P_4$	$P_1$	$T_6$	$T_{14}$	$T_{11}$
Primary	0.95	-2	4	2	4	10	70	20	14	85
Min	0.8	-10	2	1	2	5	50	15	5	75
Max	1	10	8	5	8	20	90	25	20	100
Optimized	0.99	-3.5	2.5	1.3	4	15	60	19	15	79

Table 7: Variable parameters of solid desiccant cycles in Ramsar city

Parameter	Diff Lat & Tilt	$\dot{m}_{15}$	$T_{16}$	$T_4$	$T_{in}$	$RH_n$
Primary	-2	2	85	56	23	0.5
Min	-10	1	75	45	20	0.3
Max	10	5	100	70	28	0.7
Optimized	-4	1.3	80	68	25	0.55

## 6. Results and discussion

18 In this section, annual economic indicators such as cash flow, operating costs, payback period, and  
 19 environmental emissions production index have been indicated for each climatic zone based on the  
 20 selected cooling cycle in that region. Furthermore, the return on investment is calculated using two  
 21 widely-used economic analysis methods LCC and NPV.

## 6.1. Economic and environmental evaluation results of solar cooling cycles

### 6.1.1. Semi-arid Climate (Representative city: Isfahan)

In Figure 7, the economic-environmental parameters are examined, including the annual operating cost of each cycle, the annual profitability of each cycle, and the annual CO<sub>2</sub> emission in each of the three cycles operated in Isfahan city. Each cycle's annual profitability is due to replacing fuel consumption costs with energy provided by solar collectors. Due to the equal available roof area for all cycles in this city, the annual profitability in all three cycles is a constant value of \$1040. The annual operating cost is affected by various parameters, with the most significant being gas consumption in each cycle. Notably, the highest gas consumption, and consequently the highest annual operating cost and the highest annual CO<sub>2</sub> emission, is related to the Solid Desiccant cycle in this region, with values of \$8269 and 118086 kg, respectively.

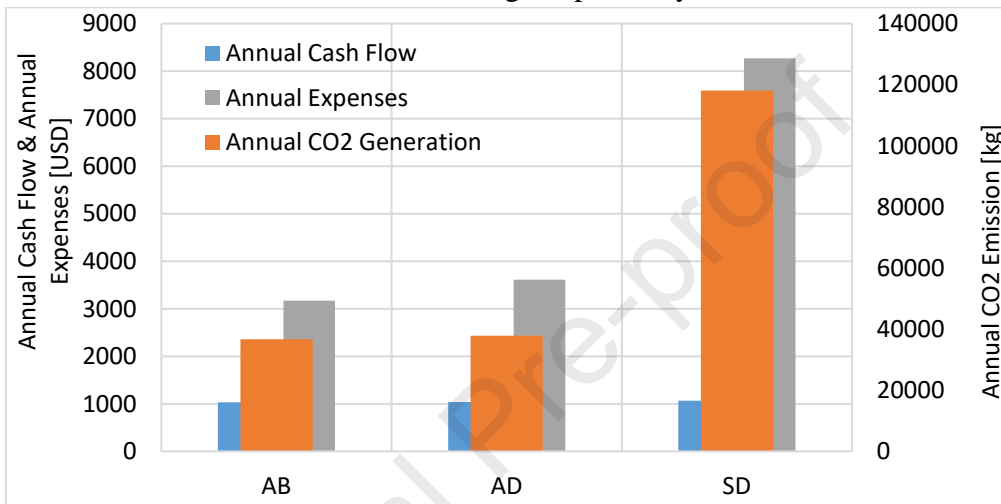


Figure 7: Annual CO<sub>2</sub> emission, Cash flow and Annual Costs of refrigeration cycles in Isfahan

Figure 8 illustrates the payback period of each solar cooling cycle for Isfahan city based on the SPP method. It can be concluded that the longest payback period is associated with the Liquid Absorption cycle, while the shortest payback period is related to the Solid Desiccant system, 10.9 and 9 years respectively. The reason is that, due to the fixed number and area of collectors that can be installed on the roof, a larger portion of the initial investment cost in the Liquid Absorption cycle is allocated to solar collectors compared to the other two systems. The shortest payback period among the examined cycles in Isfahan is for the Solid Desiccant cycle, which has a duration of 9 years.

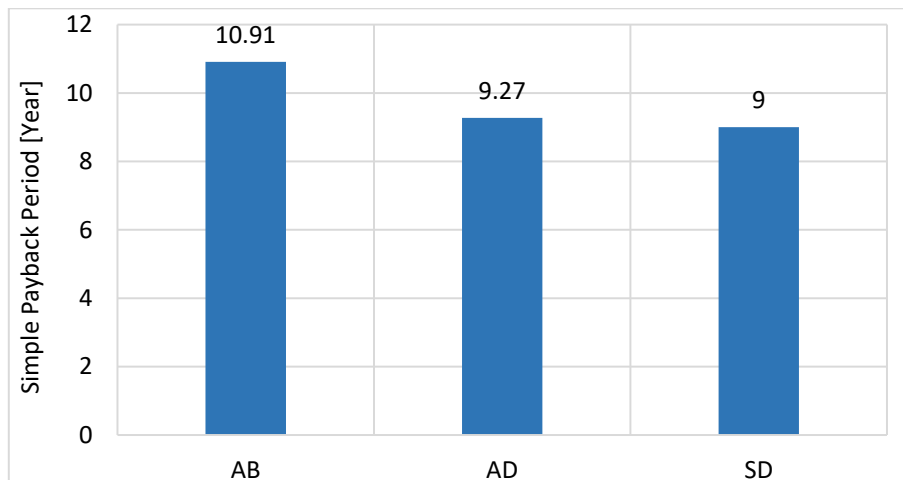
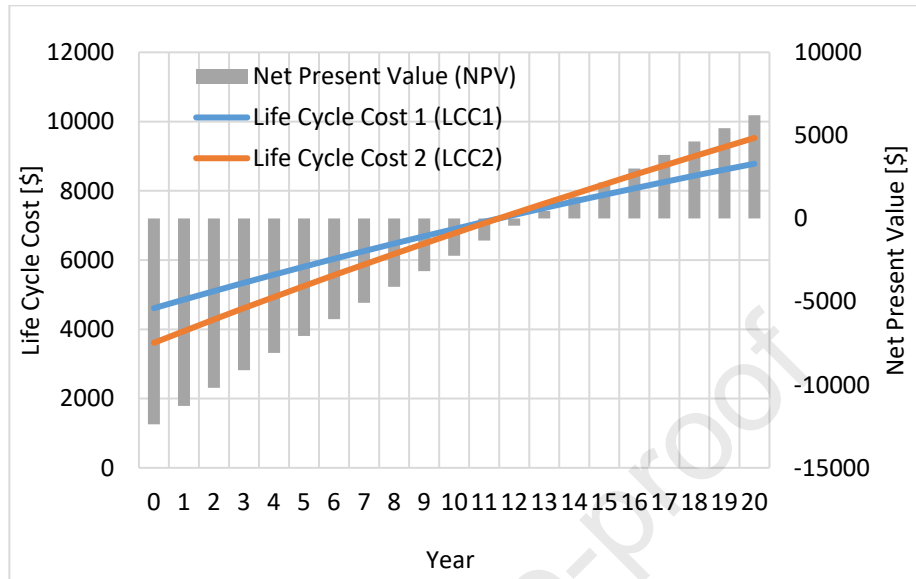


Figure 8: Comparison of payback periods in various solar cooling cycles in Isfahan city.

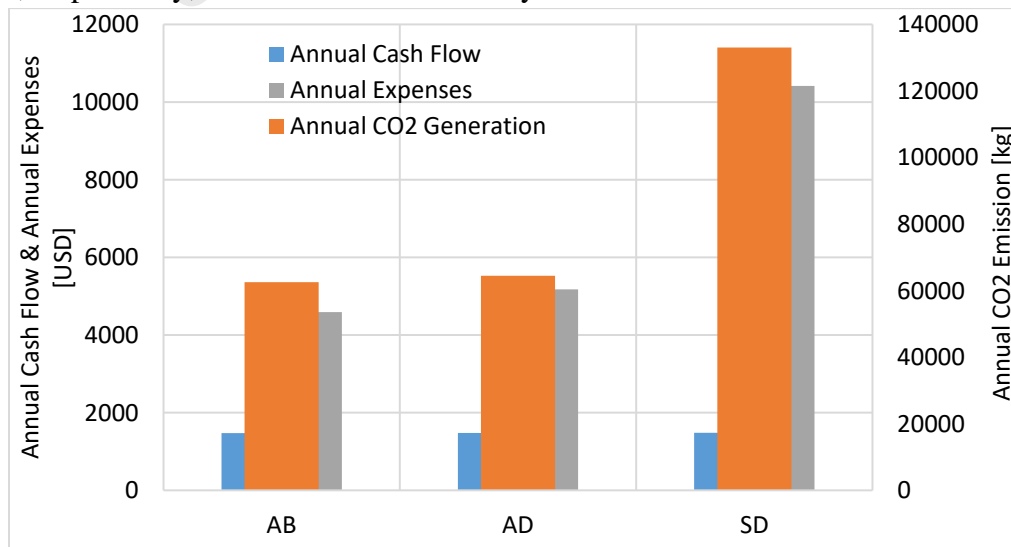
1 Figure 9 compares the system's life cycle cost for two scenarios, as mentioned in section 5.4, for the  
 2 packaged Liquid Absorption cycle in Isfahan. It can be observed that the payback period for this  
 3 cycle, considering the time when the two systems become economically equivalent in terms of life  
 4 cycle costs and the break-even point of the system based on the NPV index, is approximately 12  
 5 years.



6  
 7 Figure 9: Comparison of the system's life cycle costs for two scenarios, gas-fired and hybrid, in Isfahan city,  
 8 liquid absorption cycle.  
 9

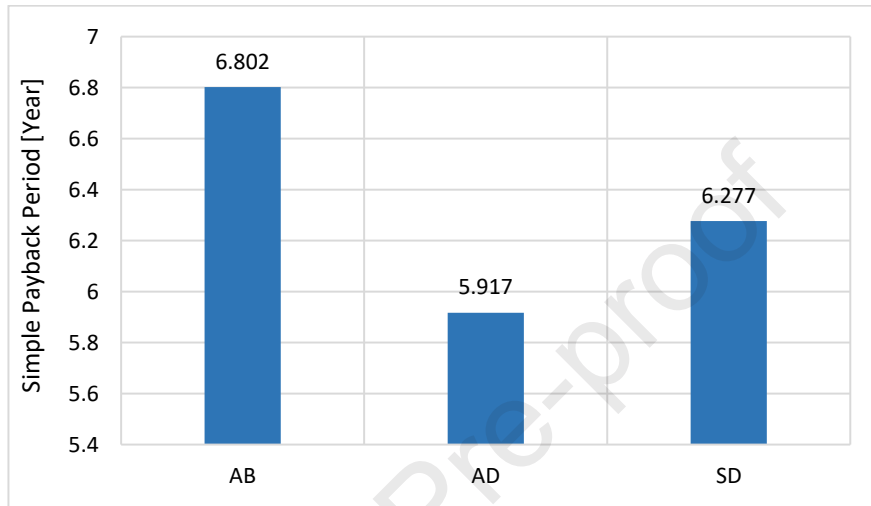
### 10 6.1.2. Warm and Dry Climate (representative city: Kerman)

11 Figure 10 compares annual costs, net profits, and the amount of environmental pollutants produced  
 12 by each cycle in Kerman city. The annual net profit resulting from using solar collectors instead of  
 13 burning gas in the heater is constant and equal to \$1,480 in all cycles due to the equal collector area  
 14 available for all cycles in this city. Regarding the amount of CO<sub>2</sub> emission and annual operating  
 15 costs, the Solid Desiccant cycle has the highest values, while the two Absorption cycles, Liquid and  
 16 Solid, have nearly equal values. The approximate values for these two parameters are 63,000 kg  
 17 and \$4,700, respectively, for the Solid Desiccant cycle.



18  
 19 Figure 10: Annual CO<sub>2</sub> emission, annual operating costs, and net annual profit for various cycles in the  
 20 Kerman city  
 21

1 Figure 11 illustrates the payback period for each solar cooling cycle in Kerman city based on the  
 2 SPP method. It can be concluded that the longest payback period is associated with the Liquid  
 3 Absorption cycle, while the shortest payback period is related to the Solid Desiccant system. This is  
 4 due to the fixed number and area of collectors that can be installed on the roof; a larger portion of  
 5 the initial investment cost in the Liquid Absorption cycle is allocated to solar collectors compared  
 6 to the other two systems. The payback period for the Solid Desiccant cycle is approximately 6  
 7 years, while the Liquid Absorption cycle has a payback period of around 6.8 years. The major  
 8 difference between these two cycles in this climate is related to the initial investment cost, which is  
 9 significantly higher in the Solid Desiccant system compared to the Liquid Absorption system.



10 Figure 11: Comparison of payback periods in solar cooling cycles in Kerman city.

11

12

13

14

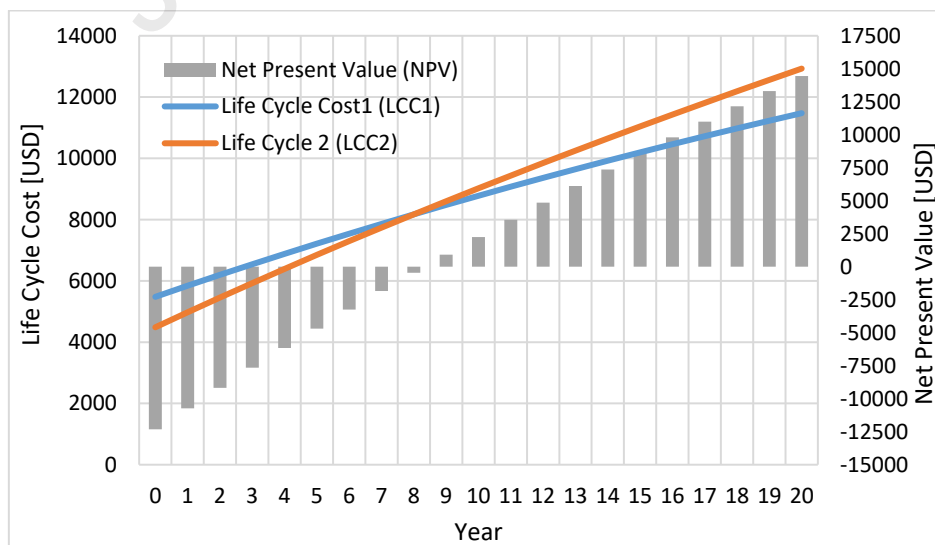
15

16

17

18

Figure 12 compares the system's life cycle cost for two scenarios, as mentioned in section 5.4, for  
 the packaged Liquid Absorption cycle in Kerman city. It can be observed that the payback period  
 for this cycle, considering the time when the two systems become economically equivalent in terms  
 of life cycle costs and the break-even point of the system based on the NPV index, falls between  
 years 7 and 8. The incident solar radiation provides a significant portion of the energy for this  
 cycle.



19

20

21

22

23

Figure 12: Comparison of system's life cycle costs for two scenarios, gas-fired and hybrid, in the Kerman  
 city, liquid absorption cycle.

### 6.1.3. Warm and Humid Climate (representative city: Bushehr)

In Figure 13, the levels of CO<sub>2</sub> emission, annual expenses, and annual profitability of each of the defined cycles in Bushehr city are compared. The annual profitability in each cycle results from utilizing solar collectors instead of gas-fired heaters. Due to the uniform building structure and available roof area for solar collector installation in all three cycles, the annual profitability for all three cycles is approximately \$1,825. The Desiccant cycle exhibits the highest CO<sub>2</sub> emission and annual expenses in this climate, with values of approximately 302,383 kg and \$24,549, respectively. It's worth noting that the values of these parameters in the other two cycles show relatively minor differences compared to the Solid Desiccant cycle.

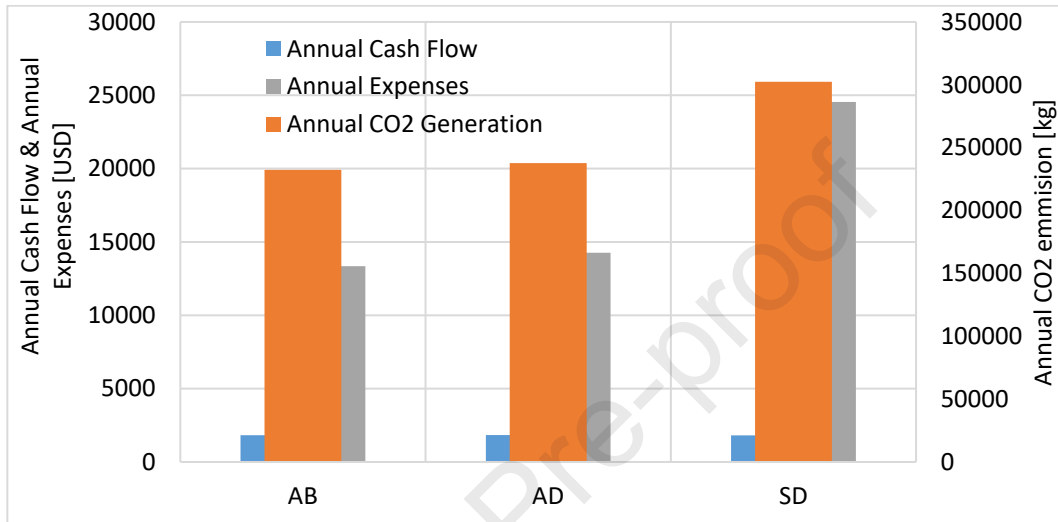


Figure 13: CO<sub>2</sub> emission, annual operating costs, and net annual profit for various cycles in Bushehr city.

10  
11  
12

Figure 14 illustrates the payback period for each solar cooling cycle in Bushehr city, using the SPP (Simple Payback Period) method. It can be concluded that the longest payback period is associated with the Liquid Absorption cycle, while the shortest payback period is attributed to the Solid Desiccant system. Given the fixed number and area of solar collectors that can be installed on rooftops, a more substantial portion of the initial capital investment cost in the liquid absorption cycle is allocated to solar collectors compared to the other two systems. The payback period for the Solid Desiccant cycle is approximately 5 years.

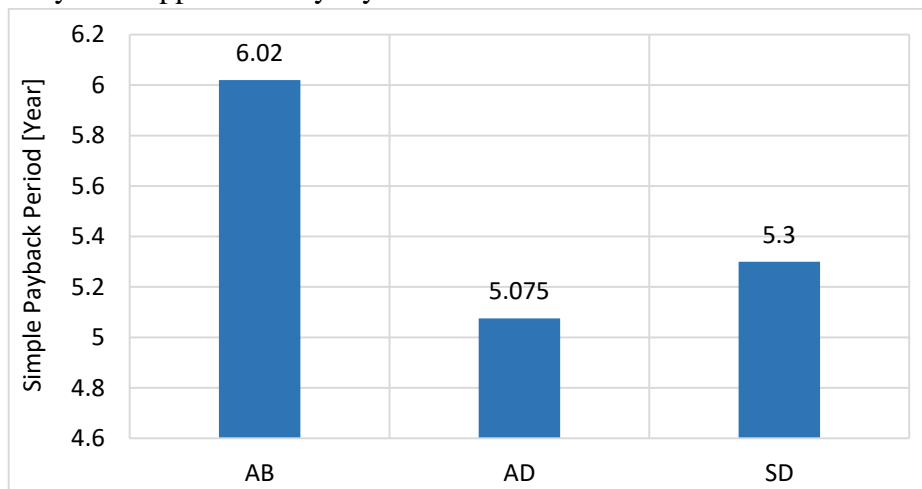
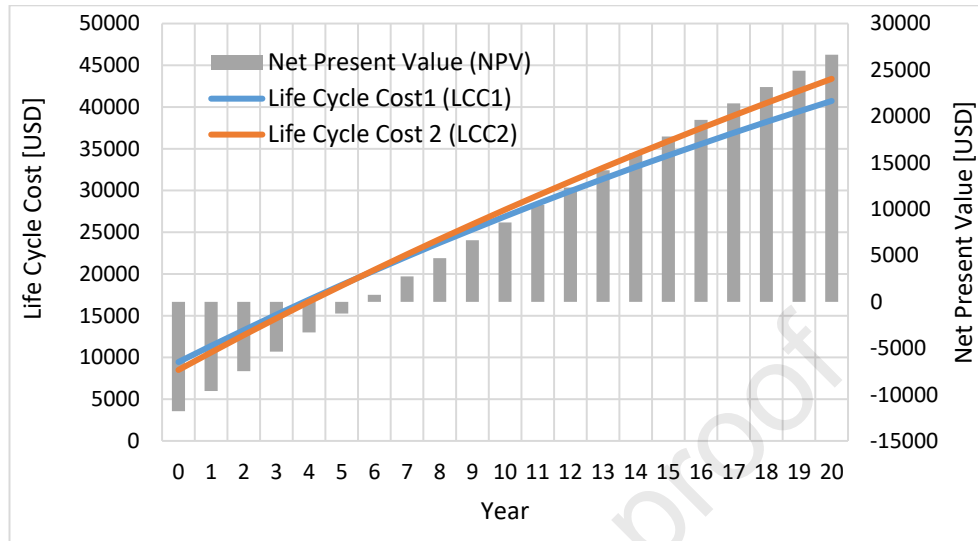


Figure 14: Comparison of payback periods in solar cooling cycles in Bushehr city.

20  
21  
22

Figure 15 compares the system's life cycle costs in two scenarios, as mentioned in section 5.4, for the Solid Desiccant cycle in Bushehr city. It can be concluded that the payback period for this

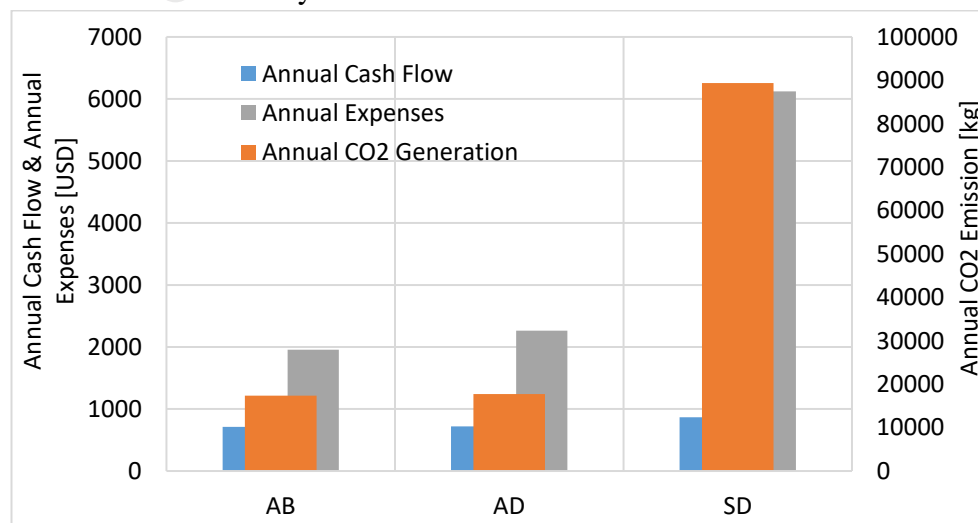
1 cycle, considering the time when the two systems achieve economic equivalence in terms of life  
 2 cycle costs and the system's break-even point based on the NPV (Net Present Value) index, is  
 3 approximately 6 years. This value is lower than that of the Liquid Absorption cycle, and this cycle,  
 4 due to its lower initial capital investment cost compared to the Solid Desiccant cycle, has the  
 5 potential to be more suitable for use in warm and humid areas.



6  
 7 Figure 15: Comparison of system's life cycle costs for two scenarios, gas-fired and hybrid, solid desiccant  
 8 cycle in Bushehr city.  
 9

#### 10 6.1.4. Cold and Mountainous Climate (representative city: Tabriz)

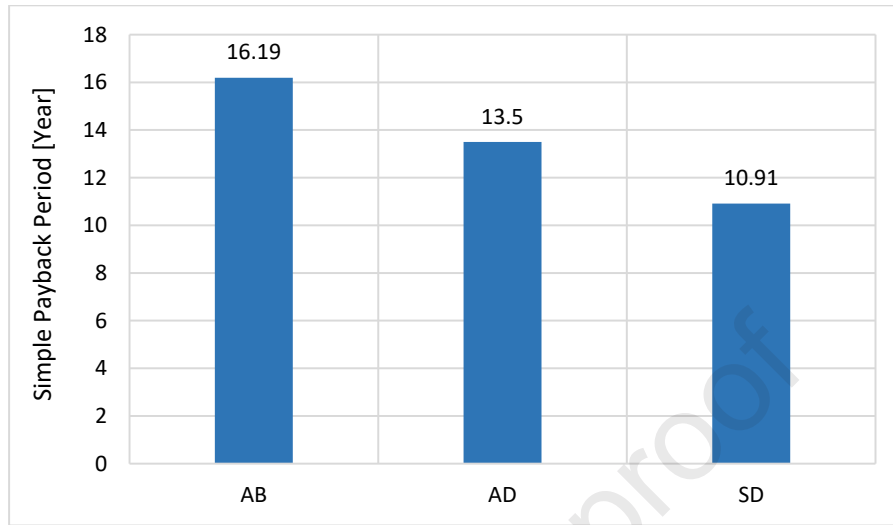
11 Figure 16 compares various economic and environmental parameters in Tabriz city, including  
 12 annual operating costs for each cycle, annual net profitability for each cycle, and CO<sub>2</sub> emission in  
 13 each cycle. In such a climate, if the Solid Desiccant cycle is used, annual operating costs and  
 14 environmental CO<sub>2</sub> emission are approximately four times higher than the absorption cycles, as  
 15 observed. The CO<sub>2</sub> emission in the Solid Desiccant cycle is 89,380 kg, in the Solid Absorption  
 16 cycle it is 17,740 kg, and in the Liquid Absorption cycle, it is 17,368 kg per year. This highlights  
 17 the significantly lower annual operating costs and fuel consumption of the absorption cycles  
 18 compared to the Solid Desiccant cycle in this climate.



19  
 20 Figure 16: CO<sub>2</sub> emission, annual operating costs, and net annual profit for various cycles in Tabriz  
 21

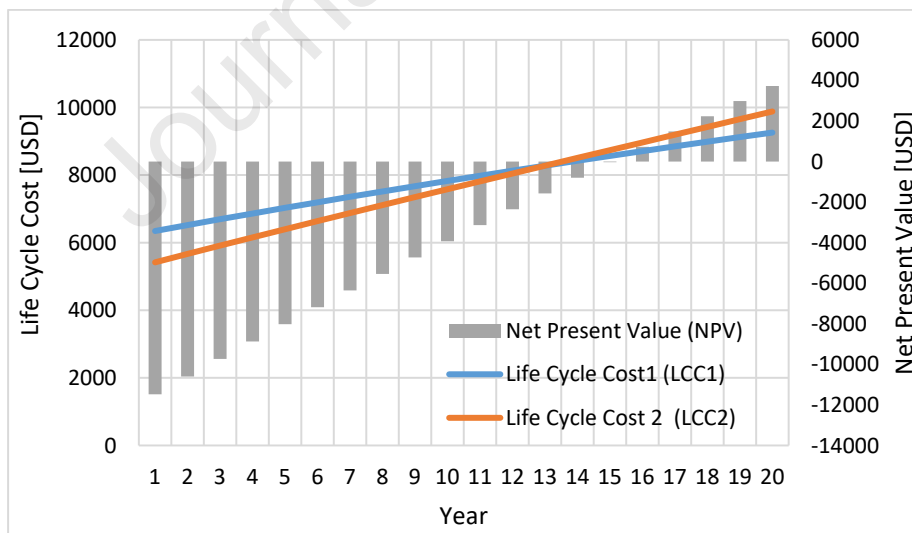
22 Figure 17 presents the payback period for each solar cooling cycle in Tabriz city, using the SPP  
 23 method. It can be inferred that the longest payback period corresponds to the Liquid Absorption

1 cycle, while the shortest payback period is attributed to the Solid Desiccant system. The payback  
 2 period difference between the Solid Desiccant and Solid Absorption cycles is approximately 30%,  
 3 and the difference between the Liquid Absorption and Solid Absorption cycles is around 30%. The  
 4 shortest payback period is attributed to the Solid Desiccant cycle, with an estimated duration of  
 5 around 11 years.



6  
7 Figure 17: Comparison of payback periods in solar cooling cycles in Tabriz city.

8  
9 Figure 18 compares the system's life cycle costs in two scenarios, as mentioned in section 5.4, for  
 10 the Solid Desiccant cycle in Tabriz city. It can be concluded that the payback period for this cycle,  
 11 considering the time when the two systems achieve economic equivalence in terms of life cycle  
 12 costs and the system's break-even point based on the NPV index, is approximately 15 years.

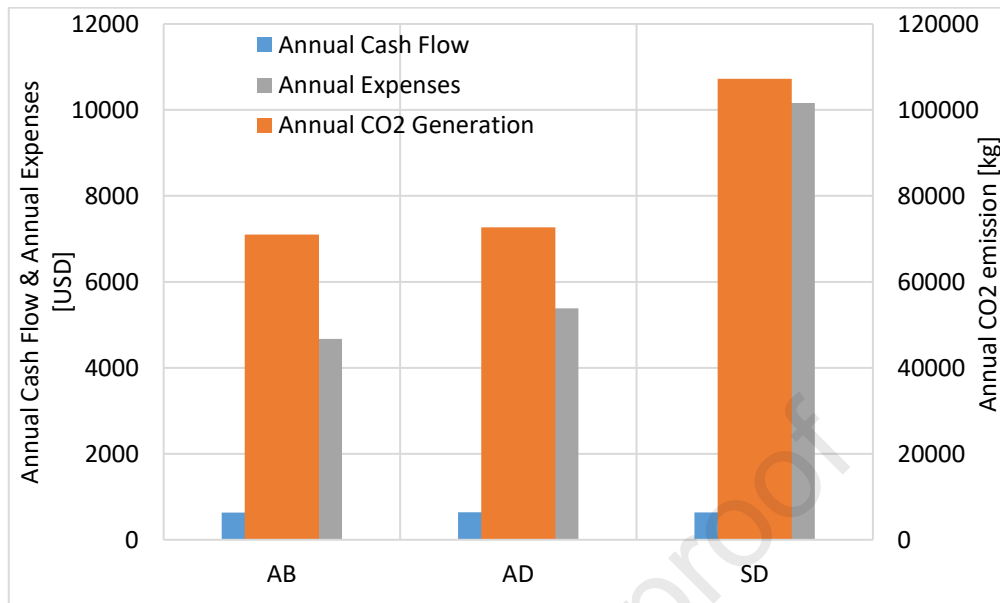


14  
15 Figure 18: Comparison of system's life cycle costs for two scenarios, gas-fired and hybrid, solid desiccant  
16 cycle in Tabriz city.

### 18 6.1.5. Moderate and Humid Climate (representative city: Ramsar)

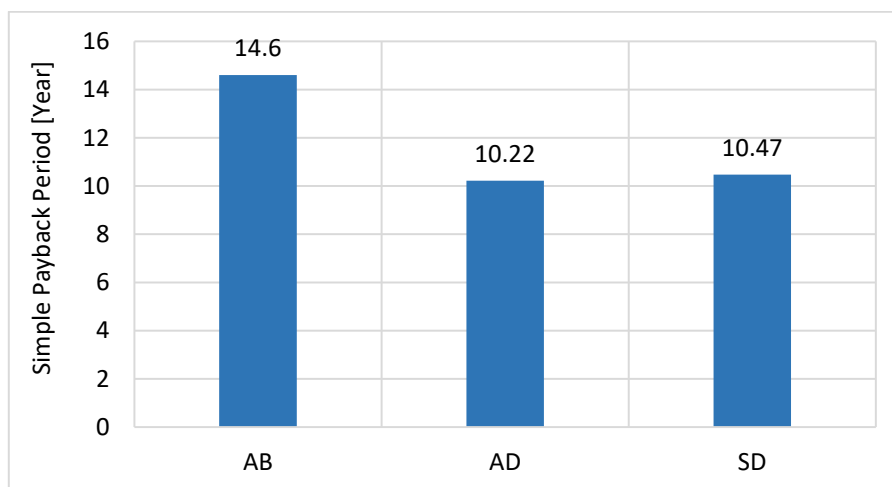
19 Figure 19 compares annual profitability indicators, annual expenses, and CO<sub>2</sub> emission levels for  
 20 various cycles in Ramsar city. In Ramsar, the profitability in all three cycles is equal due to the  
 21 uniformity of available roof area for solar collector installation in all three cycles. However, the  
 22 operational expenses of the absorption cycles and the level of toxic gas emission are almost half  
 23 that of the Solid Desiccant cycle. Considering the reasonable payback period and the ability to

1 adjust air humidity by desiccant systems, the Desiccant cycle is the preferred choice for this  
 2 climate. It has an annual operating cost of \$10,160 and emits 107,218 kg of CO<sub>2</sub> annually.  
 3



4 Figure 19: CO<sub>2</sub> emission, annual operating costs, and net annual profit for various cycles in the Ramsar city.

5  
 6  
 7 Figure 20 illustrates the payback period for each solar cooling cycle in Ramsar city, using the SPP  
 8 method. It can be concluded that the longest payback period is associated with the Liquid  
 9 Absorption cycle, while the shortest payback period is attributed to the Solid Desiccant system.  
 10 Given the fixed number and area of solar collectors that can be installed on rooftops, a more  
 11 substantial portion of the initial capital investment cost in the Liquid Absorption cycle is allocated  
 12 to solar collectors compared to the other two systems. The payback period difference between the  
 13 Solid Desiccant and Solid Absorption cycles is less than 5%, while the difference between the  
 14 Liquid Absorption and Solid Desiccant cycles is greater than 40%. Therefore, given the ability to  
 15 adjust humidity in the desiccant system and its reasonable payback period, the Solid Desiccant  
 16 system is the preferred choice in this climate.



17  
 18 Figure 20: Comparison of payback periods in solar cooling cycles in Ramsar city

19  
 20

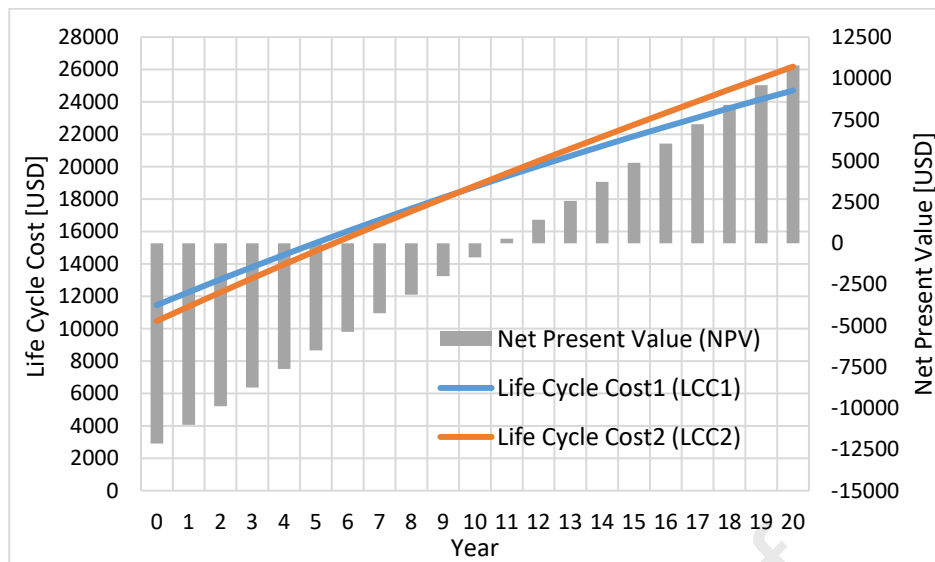


Figure 21: Comparison of the system's life cycle costs for the gas-fired and hybrid solid desiccant cycle scenarios in Ramsar city.

Figure 21 compares the system's life cycle costs in two scenarios, as mentioned in section 5.4, for the Solid Desiccant cycle in the Ramsar city. It can be concluded that the payback period for this cycle, considering the time when the two systems achieve economic equivalence in terms of life cycle costs and the system's break-even point based on the NPV index, is approximately 10 years, that is the lowest among the proposed systems for this climate. The reason is the relatively high annual fuel savings compared to this system's initial capital investment cost. Additionally, this system's initial capital investment cost is relatively high, and the surplus cost incurred to purchase the solar system compared to the total cost of the desired cooling system is very small, which is compensated in a short time frame.

## 6.2. Parametric study

The variables analyzed in this section are collector absorber area, collector tilt angle, solar collector efficiency, building cooling load, total incident solar radiation on the horizontal surface, and geographic latitude. The target indicators are energy efficiency, exergy efficiency, solar fraction, gas and primary energy consumption, gas savings, and reductions in environmental pollutants. When studying the impact of technical parameters, factors such as the required building cooling load can directly indicate changes in the building's floor area and its usage. Examining the effect of changing the efficiency of installed collectors covers various types of collectors with different efficiencies. Changing the collector absorber area implies a change in the available roof area of the building. Changes in the beam and total radiations received on the horizontal surface are equivalent to changes in the building's orientation angle relative to the south. Modifying technical parameters can have significant economic effects in addition to their impact on technical indicators. Changes in economic parameters and their effects on economic indicators can help extract suitable patterns for simulating economic conditions prevailing in Iran or other countries worldwide with different interest rates and gas and electricity costs. Therefore, economic parametric analysis can greatly assist in aligning the results more closely with the realities of our society and other countries worldwide with similar climatic patterns.

Table 8 illustrates the effects of changing the collector absorber area in each system. Increasing the collector area implies the increase in number of collector units installed on the roof or increase in

1 the available area for collector installation. It means more gained solar irradiation and  
 2 subsequently, more available heating energy for the system. Moreover, as we assumed a constant  
 3 cooling load for each hour of the day, thus the needed heating energy amount would stand  
 4 constantly too. Therefore, by increasing the solar energy gained by increasing the number of  
 5 collectors, the solar fraction increases. By increasing this parameter, the heating load on the  
 6 auxiliary heater is reduced, and the solar collector provides a higher portion of the required thermal  
 7 load. Therefore, natural gas consumption decreases, and pollutant emissions released by burning  
 8 natural gas decrease which results in lower annual cost. Furthermore, increasing the collector's area  
 9 leads to an increase in initial capital investments which increases the payback period. Increasing the  
 10 solar collector area from 100 to 200 m<sup>2</sup> results in 28% reduction in gas consumption during the hot  
 11 season for the liquid absorption cycle, 26% gas consumption reduction for the solid absorption  
 12 cycle, and a 10% gas consumption reduction for the solid desiccant absorption cycle. However, the  
 13 payback period index increases from 8.06 to 11.65 years in the liquid absorption cycle, from 9.66 to  
 14 18.89 years in the solid absorption cycle, and from 4.38 to 5.78 years in the solid desiccant cycle  
 15 due to the increase in initial capital investment costs. Moreover, increasing the number of solar  
 16 collectors means more heat loss because of the larger heat transfer surface area with surrounding.  
 17 This phenomenon decreases the energy efficiency of such systems.

18

19 Table 8: The effect of the collector absorber area on techno-economic parameters of solar cooling cycles

System	Collector Area [m <sup>2</sup> ]	Payback Period (SPP) [Year]	Annual Cost [\$]	Irreversibility [kWh]	CO <sub>2</sub> Reduction [kg/year]	Fuel Saving [m <sup>3</sup> /year]	Primary Energy [kWh]	Solar Fraction (SF)	Exergy Efficiency ( $\epsilon$ )	Energy Efficiency (COP)
Liquid Absorption	100	8.06	3827	269420	12003	5315	236253	0.3234	0.1869	0.868
	150	9.29	3410	271174	19491	8619	201657	0.5245	0.2168	0.8596
	200	11.65	3249	277138	23224	10141	185728	0.6142	0.2193	0.7968
Solid Adsorption	100	9.66	2416	133722	9842	4314	130132	0.3457	0.1779	0.6867
	150	13.49	2262	130783	13851	6009	112383	0.4772	0.1902	0.6307
	200	18.89	2231	125987	15258	6448	107781	0.5118	0.1996	0.5583
Solid Desiccant	100	4.38	25225	2267000	20006	9094	1845000	0.1338	0.1202	0.5782
	150	5.3	24549	2265000	33318	15144	1782000	0.2229	0.1228	0.5782
	200	5.787	23873	2265000	46630	21195	1718000	0.3121	0.1256	0.5782

20

21 Table 9 shows the effects of changes resulting from the collector slope angle. While increasing the  
 22 collector slope angle did not notably affect system efficiencies, it decreased the solar radiation  
 23 received on the collector due to the increased angle between the collector's normal axis and the axis  
 24 of beam radiation. As a result, the solar fraction decreases. This phenomenon causes an increase in  
 25 fuel consumption in this cycle, raising operational costs and reducing monetary savings.  
 26 Additionally, it increases the payback period, mainly due to the reduced solar radiation available  
 27 during the summer months, which necessitates maintaining a lower collector slope angle compared  
 28 to the geographic latitude. Increasing the collector slope angle from 28 to 40 degrees reduced the  
 29 exergy efficiency in the liquid absorption cycle by 0.07, increasing the payback period from 10.75  
 30 to 12 years. The change in the solid absorption cycle has a more significant impact on the payback  
 31 period, increasing it from 12.93 to 13.83 years. The smallest effect is observed in the desiccant  
 32 absorption cycle, which raises the payback period from 5.5 to 5.3 years. This effect is due to  
 33 receiving less available radiation during the summer season as the collector angle increases.

34

35

1

2 Table 9: The effect of the collector slope angle on techno-economic parameters of solar cooling cycles

System	Collector Tilt Angle [deg]	Payback Period (SPP) [Year]	Annual Cost [\$]	Irreversibility [kWh]	CO <sub>2</sub> Reduction [kg/year]	Fuel Saving [m <sup>3</sup> /year]	Primary Energy [kWh]	Solar Fraction (SF)	Exergy Efficiency (ε)	Energy Efficiency (COP)
Liquid Absorption	28	10.75	3155	270967	19692	8759	200193	0.5322	0.2173	0.8591
	34	11.27	3207	271619	19042	8319	204803	0.5078	0.2155	0.8607
	40	11.93	3268	272367	18331	7812	210114	0.4793	0.2129	0.8623
Solid Adsorption	28	12.93	2222	130830	14385	6345	108865	0.4989	0.1856	0.6251
	34	13.34	2252	131704	13992	6096	111467	0.4829	0.1852	0.6294
	40	13.82	2284	131699	13585	5827	114283	0.4653	0.1851	0.634
Solid Desiccant	28	5.33	24560	2265000	33105	15048	1783000	0.2215	0.1227	0.5782
	34	5.43	24604	2265000	32308	14686	1787000	0.2162	0.1226	0.5782
	40	5.5	24630	2265000	31825	14466	1789000	0.2129	0.1225	0.5782

3

4 Table 10 illustrates the changes in economic and technical indicators in response to variations in  
5 collector efficiency. This alteration signifies an enhancement in performance or a change in the  
6 type of collector used, resulting in an increased capacity of the collector to convert solar radiation  
7 energy into useful heat. As collector efficiency increases, the solar fraction rises, and solar thermal  
8 collectors contribute more to the heat supply. As a result, there is a decreasing trend in gas  
9 consumption and primary energy consumption, leading to an annual cost reduction associated with  
10 gas consumption. The payback period shortens with a decrease in current cycle costs and  
11 subsequent economic savings. Increasing collector efficiency from 40% to 80% can result in a  
12 substantial reduction in fuel consumption and an increase in exergy efficiency. In the liquid  
13 absorption cycle, exergy efficiency increases from 0.185 to 0.218, fuel consumption decreases from  
14 5067 to 9355 m<sup>3</sup> per year, and the payback period decreases from 15 to 8.4 years. Similarly, in the  
15 solid absorption cycle, a 2% increase in exergy efficiency reduces the payback time from 18 to 13  
16 years. In the solid desiccant cycle, natural gas consumption savings become twofold, reducing the  
17 payback period from 8.15 years to 4.75 years.

18

19 Table 10: Effect of collector efficiency on the techno-economic parameters of solar cooling cycles.

System	Collector Efficiency	Payback Period (SPP) [Year]	Annual Cost [\$]	Irreversibility [kWh]	CO <sub>2</sub> Reduction [kg/year]	Fuel Saving [m <sup>3</sup> /year]	Primary Energy [kWh]	Solar Fraction (SF)	Exergy Efficiency (ε)	Energy Efficiency (COP)
Liquid Absorption	0.4	14.94	3913	269354	11443	5067	238851	0.3083	0.185	0.8681
	0.6	10.46	3558	270256	17026	7538	212982	0.4592	0.2072	0.867
	0.8	8.64	3309	272843	21219	9355	193956	0.5681	0.2182	0.8403
Solid Adsorption	0.4	17.95	2490	133907	9383	4113	132236	0.3295	0.1748	0.6869
	0.6	14.18	2307	133884	12924	5640	116247	0.4491	0.1893	0.6583
	0.8	13.12	2236	128984	14481	6227	110094	0.4941	0.194	0.6226
Solid Desiccant	0.4	8.148	25327	2267000	19055	8661	1850000	0.1274	0.1201	0.5782
	0.6	6	24808	2266000	28563	12983	1804000	0.1911	0.1218	0.5782
	0.8	4.74	24289	2265000	38072	17305	1759000	0.2548	0.1237	0.5782

20

21 Table 11 illustrates the impact of variations in the building cooling load on solar cooling cycles'  
22 technical and economic parameters. A change in the building cooling load refers to alterations in  
23 the building's floor area or usage. With an increase in the building cooling load, the required heat  
24 load of the cycle will not increase significantly. Consequently, the constant chiller capacity  
25 achieves a greater cooling effect, resulting in improved system efficiency. Increasing the building

1 cooling load also increases the heat load required in generators, hot beds, and hot coils. Given the  
 2 constant solar radiation received, this increase is compensated for by an auxiliary heater, resulting  
 3 in a decreasing solar fraction. An increase in the heater load implies higher primary energy  
 4 consumption and, as a result, increased pollutant emissions.

5

6 Table 11: The effect of building cooling load on the techno-economic parameters of solar cooling cycles.

System	Cooling Load Coefficient	Payback Period (SPP) [Year]	Annual Cost [\$]	Irreversibility [kWh]	CO <sub>2</sub> Reduction [kg/year]	Fuel Saving [m <sup>3</sup> /year]	Primary Energy [kWh]	Solar Fraction (SF)	Exergy Efficiency (ε)	Energy Efficiency (COP)
Liquid Absorption	0.7	14	2420	193322	16369	7138	147775	0.6176	0.2102	0.7917
	1	10.9	3171	271172	19491	8619	201657	0.5245	0.2203	0.8596
	1.3	10	4077	351503	19911	8815	269043	0.4129	0.2301	0.8674
Solid Adsorption	0.7	19.3	1800	86177	10726	4524	88646	0.513	0.1644	0.5535
	1	13.5	2262	130783	13851	6009	112383	0.4772	0.1852	0.6307
	1.3	11	2798	175682	15765	6898	142360	0.4237	0.1921	0.6736
Solid Desiccant	0.7	5.8	21227	1837000	41646	15144	1596000	0.2229	0.0985	0.4221
	1	5.2	24549	2265000	48411	17604	1782000	0.2174	0.1228	0.5782
	1.3	4.8	27870	2696000	52063	18932	1967000	0.201	0.1416	0.7221

7

8 Furthermore, as mentioned earlier, increasing the building cooling load reduces heat losses in the  
 9 cycle. Additionally, during some hours when all the energy required for the cycle is supplied by the  
 10 collector, maximizing the capacity of the collectors can reduce heater usage, leading to greater  
 11 savings during the warm period and subsequently reducing the payback period. This savings results  
 12 in a shorter payback period. Moreover, increasing the building cooling load will increase the initial  
 13 capital investment required to purchase a higher-capacity cooling system. In contrast to the  
 14 previous effect, this increase in initial capital investment will extend the payback period. By  
 15 increasing the building cooling load or the floor area by only 30%, all systems' energy and exergy  
 16 efficiencies increase by approximately 1%. Consequently, the payback period decreases by 1 year  
 17 for the liquid absorption cycle, 2.5 years for the solid absorption cycle, and 0.5 years for the solid  
 18 desiccant cycle.

19 Table 12 illustrates the impact of variations in total solar irradiation intensity on the performance  
 20 parameters of different cooling cycles using solar collectors. Changes in solar irradiation are  
 21 associated with altering the orientation of the building or solar collector relative to the south (as  
 22 seen in Iran). An increase in solar irradiation results in higher heat gains for the solar collectors,  
 23 thereby increasing the solar fraction, while the cooling load and heat demand remain relatively  
 24 constant.

25 As solar fraction increases due to the rise in solar irradiation, the demand for the auxiliary heater  
 26 diminishes, leading to a reduction in natural gas consumption until it reaches zero. This decrease in  
 27 auxiliary heating demand also lowers the primary energy requirements of the cooling cycles,  
 28 primarily due to the reduced use of natural gas during hotter periods. Consequently, optimizing the  
 29 orientation of solar collectors is a critical and cost-effective strategy for enhancing economic  
 30 performance and reducing natural gas consumption, alongside environmental benefits.

31 In Isfahan, a 60% increase in solar radiation, when using a liquid absorption cooling system,  
 32 reduces primary energy consumption by 15%, increases exergy efficiency by 2%, and leads to  
 33 annual fuel savings from 7,485 m<sup>3</sup> to 22,872 m<sup>3</sup>. Correspondingly, carbon emissions in this system  
 34 decrease from 19,491 kg to 22,872 kg annually. In a solid adsorption cycle, this increase in solar  
 35 radiation leads to a 1.5% rise in exergy efficiency and reduces carbon emissions from 13,851 kg to

1 15,354 kg annually. A 30% increase in radiation intensity in the solid desiccant cycle results in  
 2 annual natural gas savings from 15,144 m<sup>3</sup> to 19,527 m<sup>3</sup>. Across all cooling cycles, a 30% increase  
 3 in solar irradiation on collector surfaces shortens the payback period by one year, due to these  
 4 efficiency improvements.

5

6 Table 12: The effect of total incident radiation intensity on techno-economic parameters of cooling cycles.

System	<u>Total Irradiation Coefficient</u>	<u>Payback Period (SPP) [Year]</u>	<u>Annual Cost [\$]</u>	<u>Irreversibility [kWh]</u>	<u>CO<sub>2</sub> Reduction [kg/year]</u>	<u>Fuel Saving [m<sup>3</sup>/year]</u>	<u>Primary Energy [kWh]</u>	<u>Solar Fraction (SF)</u>	<u>Exergy Efficiency (ε)</u>	<u>Energy Efficiency (COP)</u>
Liquid Absorption	0.7	12.4	3307	271307	17210	7485	217861	0.4493	0.2065	0.8571
	1	10.91	3171	271174	19491	8619	201657	0.5245	0.2167	0.8678
	1.3	9.3	2975	273689	22872	10255	184537	0.6186	0.2244	0.8721
Solid Adsorption	0.7	14.49	2325	131674	12776	5485	117871	0.4385	0.1814	0.6397
	1	13.5	2262	130783	13851	6009	112383	0.4772	0.2056	0.6527
	1.3	12.36	2178	125344	15354	6709	105054	0.5264	0.2207	0.6611
Solid Desiccant	0.7	6.76	25030	2266000	24494	11134	1824000	0.1637	0.1211	0.5782
	1	5.32	24549	2265000	33318	15144	1782000	0.2229	0.1228	0.5782
	1.3	4.28	24023	2265000	42959	19527	1736000	0.2875	0.1248	0.5782

7

8 Table 13 examines the impact of changes in the unit cost of consumed gas on economic indicators.  
 9 With an increase in the unit cost of consumed gas, despite the fact that the annual operating costs of  
 10 the systems increase each year, savings in gas consumption are achieved in the hybrid cooling  
 11 system. The financial value of these savings increases annually, resulting in a larger portion of the  
 12 initial investment being recovered each year. Ultimately, the payback period and, consequently, the  
 13 government subsidies will decrease. An increase in the natural gas rate from 10 to 20 cents per  
 14 cubic meter leads to an approximately 50% reduction in the payback period index in solar cooling  
 15 cycles and a 37% reduction in government subsidies in the liquid absorption cooling cycle. This  
 16 reduction in the solid absorption cycle is 24%, and in the solid desiccant cycle, it is 56%.

17

18

Table 13: The effect of unit cost of natural gas on the techno-economic parameters

System	<u>Natural Gas Unit Price [\$]</u>	<u>Payback Period (SPP) [Year]</u>	<u>Annual Saving [\$]</u>	<u>Annual Subsidy [\$]</u>	<u>Annual Cost [\$]</u>
Liquid Absorption	0.1	12.87	861.9	1833	2902
	0.14	9.473	1207	1561	3440
	0.2	6.787	1724	1152	4247
Solid Adsorption	0.1	15.53	600.9	1958	2133
	0.14	11.93	841.2	1768	2393
	0.2	8.853	1202	1483	2782
Solid Desiccant	0.1	8.548	971.5	1362	15047
	0.14	6.669	1360	1055	18017
	0.2	5.016	1943	594.6	22471

19

20 Table 14 shows the impact of changes in the interest rate. This parameter only affects government  
 21 subsidies and the payback period calculated using the NPV method. These two indicators have a  
 22 direct relationship with each other, such that an increase in the payback period leads to an increase  
 23 in government subsidies. With an increase in the interest rate, the annual financial value of gas  
 24 savings increases. Consequently, the process of recovering the initial capital cost will accelerate,  
 25 reducing the payback period and, as a result, decreasing government subsidies to users. This factor

1 can significantly incentivize using solar systems and renewable energy sources, especially in  
 2 countries with high-interest rates. In this regard, a higher interest rate shortens the payback period  
 3 for these systems. An increase in the interest rate from 5% to 10% has a positive impact, reducing  
 4 the payback period by approximately 0.5 years for the closed-loop liquid absorption cycle, reducing  
 5 it by 2 years for the closed-loop solid absorption cycle, and reducing it by almost 1 year for the  
 6 closed-loop solid desiccant cycle. On average, this increase in the interest rate can reduce  
 7 government subsidies to users by up to 2%.

8 Table 14: The effect of interest rate on the techno-economic parameters of solar cooling cycles.

System	Interest Rate	Payback Period (NPV) [Year]	Annual Subsidy [\$]
Liquid Absorption	0.05	12.5	1697
	0.08	12.2	1693
	0.1	11.9	1689
Solid Adsorption	0.05	15.3	1863
	0.08	14.22	1855
	0.1	13.32	1847
Solid Desiccant	0.05	8.31	1209
	0.08	7.74	1193
	0.1	7.42	1177

9  
 10 Table 15 shows the impact of changes in solar collectors' initial capital investment cost.  
 11 Technological advancements in solar thermal collectors over the past decade have led to a  
 12 significant increase in efficiency and a notable reduction in initial costs. Solar collectors represent a  
 13 substantial portion of the initial capital investment in solar cooling systems. Therefore, with the  
 14 growth in industries related to solar systems, it seems that the cost of these collectors will decrease  
 15 by more than 50% in the next 5 years. With a reduction in solar collectors' initial capital investment  
 16 cost in solar cooling cycles, the payback period will also significantly decrease, leading to a  
 17 corresponding reduction in government subsidies to users. The results show that a reduction in the  
 18 capital investment cost of solar collectors by up to 75% compared to the current state can bring  
 19 government subsidies for reducing the payback period to less than 4 years in closed-loop liquid and  
 20 solid absorption cycles and up to 50% in the closed-loop solid desiccant cycle. Furthermore,  
 21 reducing the initial capital investment cost in solar systems by 50% less than the current state can  
 22 reduce the payback period based on NPV in liquid absorption, solid absorption, and desiccant solar  
 23 cycles by 6.7, 7.8, and 4.9 years, respectively.

24  
 25 Table 15: The effect of the initial capital investment cost of solar collectors on the economic parameters

System	Solar Collector Cost Reduction [%]	Payback Period (NPV) [Year]	Payback Period (SPP) [Year]	Annual Subsidy [\$]	Annual Saving [\$]
Liquid Absorption	Primary Case	12.5	10.9	1695	1034
	25	8.7	7.962	1020	1034
	50	5.84	5.164	342.4	1034
	75	2.86	2.507	0	1034
Solid Adsorption	Primary Case	15.3	13.5	2093	543
	25	10.51	9.783	1185	721.1
	50	6.8	6.307	507.9	721.1
	75	3.05	3.045	0	721.1
Solid Desiccant	Primary Case	8.3	5.2	874	1753
	25	6.71	4.416	531.2	1166
	50	3.49	3.419	0	1166
	75	1.52	1.495	0	1166

### 6.3. Multi-objective optimization results

In this section, the multi-objective optimization results are presented separately for each criterion. Figure 22 compares the energy efficiency of each cycle in both the initial and optimized states. It is noticeable that, through this optimization, the energy efficiency has increased by approximately 5.5% in Isfahan City by using liquid absorption cycle, around 3.5% in Kerman City by using liquid absorption cycle, about 16.6% in Bushehr City by using solid desiccant cycle, approximately 5% in Tabriz City by using solid adsorption cycle, and roughly 14% in Ramsar City by using solid desiccant cycle. The reason for this increase in energy efficiency is the selection of optimal values for flow rates in each cycle, as well as the optimal selection of the inlet hot fluid temperature to the generator in the liquid absorption cycle, the optimal selection of pressures for adsorbents in the solid adsorption cycle, and additionally, the choice of the optimal exit temperature of the desiccant wheel in the solid desiccant cycle. Furthermore, the highest level of optimization effectiveness, in terms of energy efficiency, has been achieved for the liquid absorption cycles, while the lowest improvement is observed in the solid adsorption cycle.

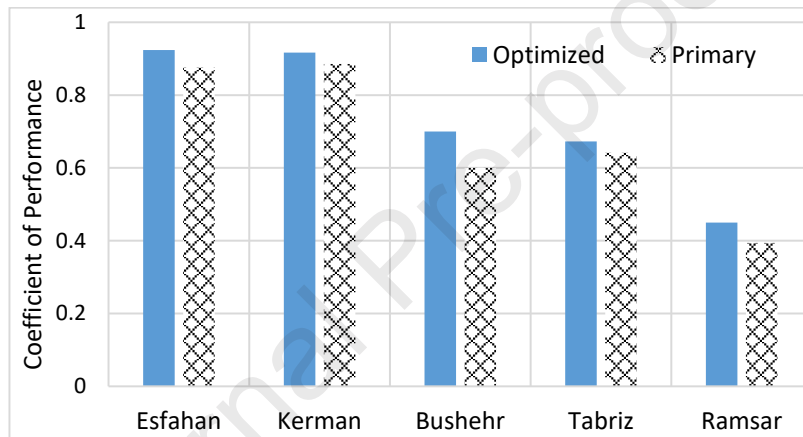


Figure 22: COP of selected cycles in different climates in both optimized and primary case studies

In Figure 23, a comparison of the exergy efficiency of each cycle in both the initial and optimized states is provided. Exergy efficiency is one of the crucial indicators in decision-making for the system's operability, and in this optimization case, it has shown an increasing trend in all climates. In Isfahan City, this increase is approximately 18.6% due to using the liquid absorption cycle, in Kerman City, about 22.6% using liquid absorption cycle, in Bushehr City about 26.4% by using solid desiccant cycle, in Tabriz City approximately 17.3% by using solid adsorption cycle, and in Ramsar City, it is around 18% by using solid desiccant cycle. The improvement in exergy efficiency in the absorption cycles is attributed to the optimal selection of high and low cycle pressures, leading to a reduced pressure difference. Additionally, in all cycles, the optimized reduction in the flow rate of the hot fluid significantly mitigates exergy destruction, resulting in an overall increase in system exergy efficiency. Notably, the highest degree of optimization in terms of exergy efficiency is related to the solid desiccant cycle in Bushehr City, while the least variation due to optimization is associated with the solid adsorption cycle in Tabriz City.

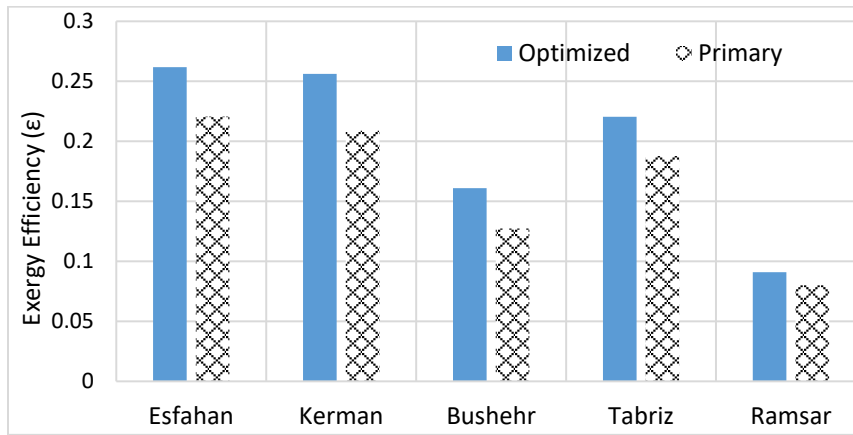


Figure 23: Comparison of the exergy efficiency of selected cycles in different climates in both optimized and initial states.

In Figure 24, a comparison of the required primary energy for selected cycles in each city in both the optimized and primary case studies is presented. The optimization results show that the reduction in primary energy consumption in the solid desiccant cycle in Bushehr City is more noticeable compared to other cycles, while the least reduction is observed in the solid adsorption cycle in Tabriz City. The reduction in primary energy consumption in the liquid absorption cycle in Isfahan City is about 13%, in Kerman City with liquid absorption cycle of about 16%, in Bushehr City about 17%, in Tabriz City about 6%, and in Ramsar City by using solid desiccant cycle, with the solid desiccant cycle, it is about 10%. Additionally, through the adjustment and optimization of the slope angle of solar collectors, the received solar radiation on the collector surface increases. This increase in received radiation also enhances the heat production in the collector. Consequently, with the increased thermal load generated by the collector, the imposed load on the heater, fuel consumption, and primary energy consumption decrease.

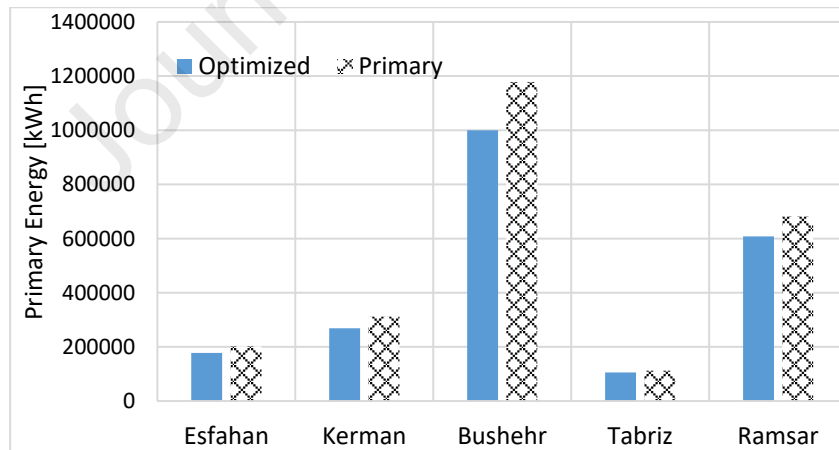
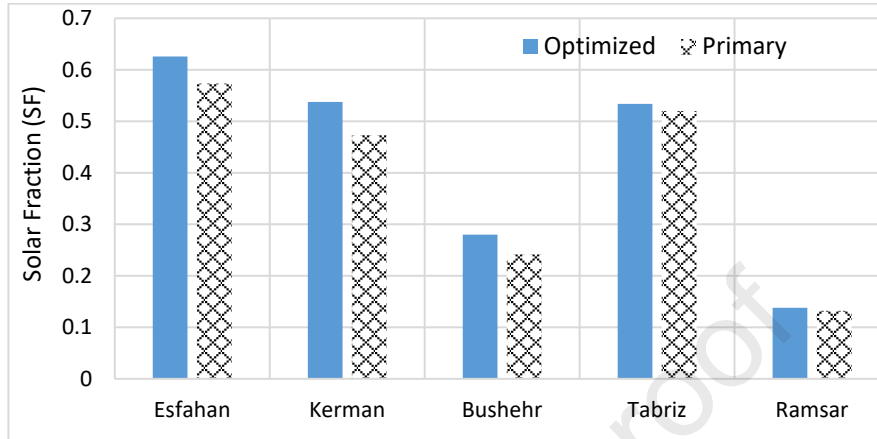


Figure 24: Comparison of the primary energy for selected cycles in different climates in both optimized and primary cases

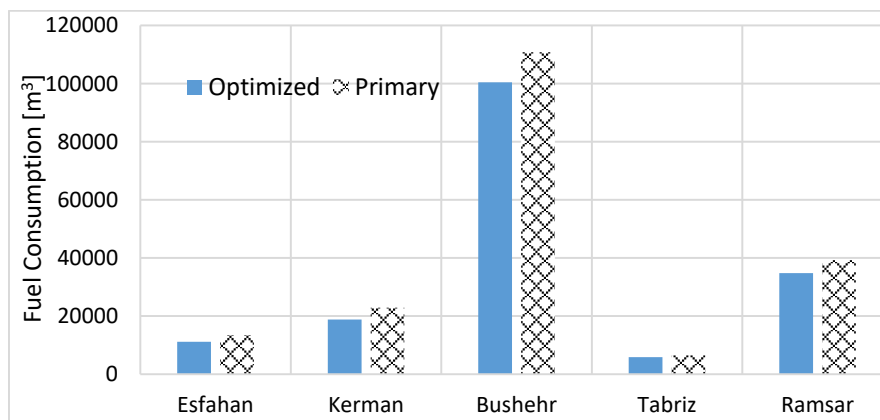
Figure 25 compares the solar fraction in different cities in baseline and optimized states. The solar fraction has increased in all cities during this optimization process. However, the increase in this parameter is much more significant in the solid desiccant cycle in Bushehr City compared to other cycles. In Isfahan City, the increase is approximately 9.1% due to using liquid absorption cycle, in Kerman City, about 13.6% using liquid absorption cycle, in Bushehr City, about 15.9% by using solid desiccant cycle, in Tabriz City, about 2.7% using solid adsorption cycle, and in Ramsar City about 4.5% by solid desiccant cycle. The solar fraction is influenced by two factors: solar radiation

1 received directly affects this parameter and increases it by optimizing the slope angle of the  
 2 collector and receiving a greater amount of solar radiation. The other factor is the required thermal  
 3 energy of the cycle, which inversely affects this parameter. By reducing the flow rate of hot water  
 4 and adjusting it to an optimal level, the overall thermal energy required by the cycle decreases and  
 5 can increase the value of this solar fraction.  
 6



7  
 8 Figure 25: Comparison of the solar fraction for selected cycles in different climates for optimized and  
 9 baseline case studies  
 10

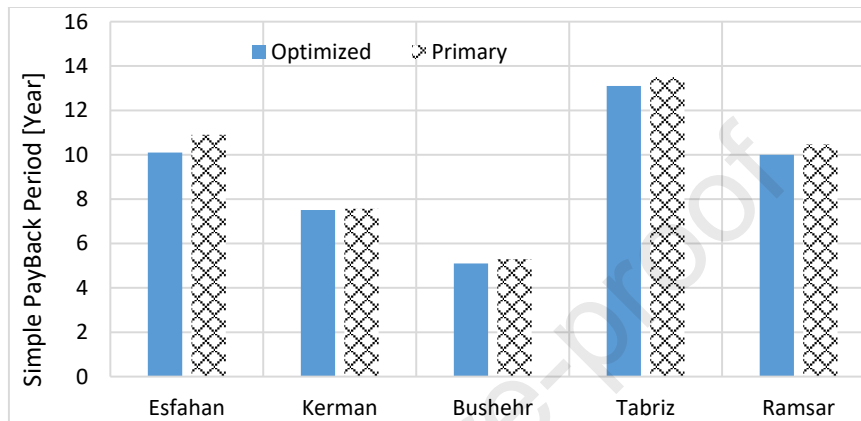
11 Figure 26 compares fuel consumption in various cycles in both baseline and optimized states. Due  
 12 to the increased energy efficiency of the systems used in different cities, fuel consumption has also  
 13 decreased. Liquid absorption cycles show a more significant reduction in fuel consumption than  
 14 other cycles. The reduction in fuel consumption after optimization is approximately 20% in Isfahan  
 15 City using liquid absorption, 22% in Kerman City using liquid absorption cycle, 10% in Bushehr  
 16 City by using solid desiccant cycle, about 11% in Tabriz City using solid adsorption, and 11.4% in  
 17 Ramsar City using optimized solid desiccant cycle. Optimizing the slope angle of solar collectors is  
 18 among the contributing factors to this reduction. By optimizing the slope angle, it is possible to  
 19 extract maximum thermal energy from the collector unit's surface area. While keeping the required  
 20 thermal energy for the cycle constant to create a specific cooling load, the thermal load on the  
 21 heater and, consequently, fuel consumption decreases.  
 22



23  
 24 Figure 26: Comparison of fuel consumption in selected cycles in different climates for optimized and  
 25 baseline case studies  
 26

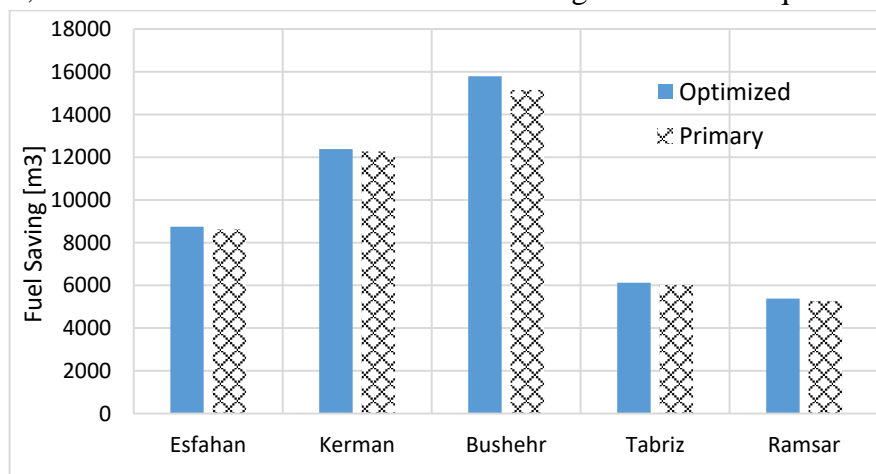
27 Figure 27 compares the payback period in different cities in baseline and optimized states. Due to  
 28 the increase in cost savings resulting from optimization, the payback period for various cycles will

1 show a decreasing trend. This reduction is approximately 8% in Isfahan City in case of using liquid  
 2 absorption cycle, almost 1% in Kerman City using liquid absorption cycle, 4% in Bushehr City by  
 3 using solid desiccant cycle, 3% in Tabriz City using solid adsorption cycle, and 4.7% in Ramsar  
 4 City by using optimized solid desiccant cycle. It is noticeable that the most significant reduction in  
 5 payback time is related to Bushehr City with the solid desiccant cycle. The optimization carried out  
 6 has the inverse effect on the annual operating costs of the cycle, reducing them. Furthermore, this  
 7 optimisation increases annual cost savings due to the reduction in the cooling exergy cost in the  
 8 power generation unit. This increased cost savings can quickly cover the initial capital investment  
 9 and effectively compensate for it.



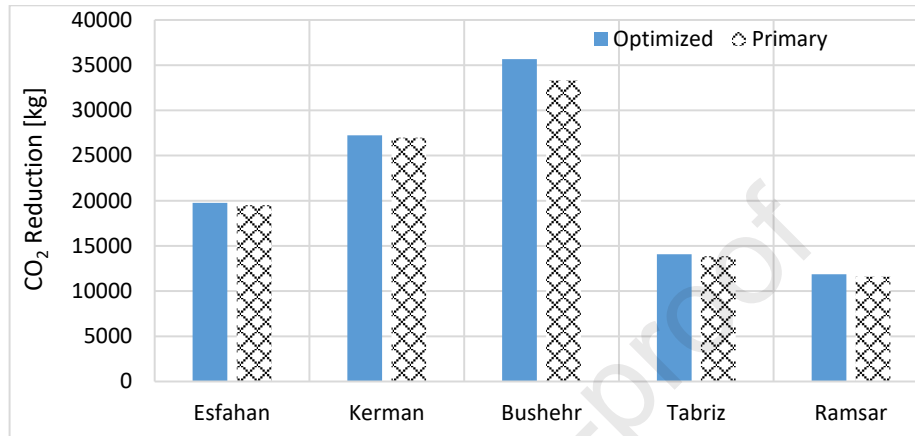
10  
 11 Figure 27: Comparison of the payback period in selected cycles in different climates for optimized and  
 12 baseline case studies  
 13

14 Figure 28 compares fuel consumption savings in different cities in baseline and optimized states.  
 15 Due to the adjustment of the collector slope angle, fuel consumption savings have also shown an  
 16 increasing trend, although this increase did not amount to a significant value. The increase in fuel  
 17 consumption savings after optimization is approximately 1.5% in Isfahan City using liquid  
 18 absorption cycle, nearly 1% in Kerman City using liquid absorption cycle, 4% by using solid  
 19 desiccant cycle in Bushehr City, 1.8% in Tabriz City using solid adsorption cycle, and  
 20 approximately 2.2% in Ramsar City using solid desiccant cycle. It should be mentioned that despite  
 21 the small percentage of savings achieved in the optimized state for each cycle, considering the very  
 22 high fuel consumption in these cycles and the widespread adoption of solar cooling cycles in the  
 23 residential sector, the numerical value of these annual savings will become quite substantial.



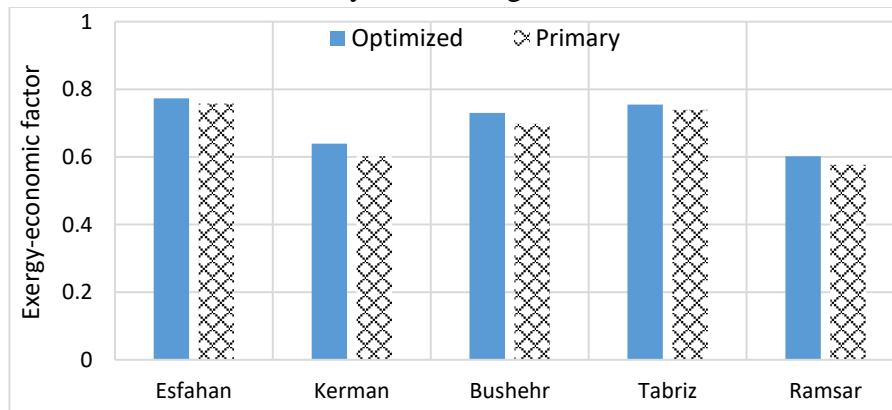
24  
 25 Figure 28: Comparison of fuel consumption savings in selected cycles in different climates for optimized  
 26 and baseline case studies.

1 Figure 29 compares the reduction in CO<sub>2</sub> emissions in each city in both the baseline and optimized  
 2 states. The pattern of changes in this indicator aligns precisely with the level of fuel consumption  
 3 savings and changes proportionally. Therefore, the reduction in carbon dioxide (CO<sub>2</sub>) emissions  
 4 compared to the primary case study after optimization is approximately 1.5% in Isfahan City by  
 5 using liquid absorption cycle, around 1% in Kerman City due to using liquid absorption cycle, 4%  
 6 in Bushehr City using optimized solid desiccant cycle, 1.8% in Tabriz City using solid adsorption  
 7 cycle, and nearly 2.2% in Ramsar City using solid desiccant cycle.  
 8



9  
 10 Figure 29: Comparison of the reduction in CO<sub>2</sub> emissions in selected cycles in different climates for  
 11 optimized and baseline case studies.  
 12

13 Figure 30 compares the exergy-economic factor in selected cycles in various climate regions of Iran  
 14 in both the optimized and primary case studies. Generally, due to the optimization based on  
 15 improving exergy-economic factors, all cycles in all cities under investigation show an increasing  
 16 trend in this indicator compared to the primary case study. Optimizing exergy-economic factors has  
 17 a distinct advantage, resulting in technical and economic indicators simultaneously contributing to  
 18 improving cycle performance. With the optimization considered, the role of using solar collector  
 19 systems to provide hot water for consumption in the cycles becomes more prominent than in the  
 20 primary case study. Since the cost of exergy from the heat generated by this method is zero, it  
 21 reduces the overall exergy cost of the cooling effect and significantly increases the exergy-  
 22 economic factor of the cycles. This increase, compared to the initial state, is approximately 2% in  
 23 Isfahan City in the case of using liquid absorption cycle, 5.8% in Kerman City using liquid  
 24 absorption cycle, 4.4% in Bushehr City using solid desiccant cycle, 2% in Tabriz City using solid  
 25 adsorption cycle, and 4.3% in Ramsar City considering the use of the solid desiccant cycle.



26  
 27 Figure 30: Comparison of the exergy-economic factor in selected cycles in different climate regions for  
 28 optimized and baseline case studies.

## 7. Conclusions

This study analyses the effectiveness of solar-thermal cooling systems in five different climatic regions of Iran. The study includes environmental-economic analysis, parametric analysis, exergy-economic analysis, and multiobjective optimization. Three refrigeration systems were simulated in all five regions: liquid absorption, solid adsorption, and closed desiccant cycles. The results showed that solar-thermal cooling systems can provide cooling during peak midday hours, and collectors produce heat energy at maximum efficiency. Technical and environmental-economic analyses were conducted, followed by parametric analysis and optimization. The following concludes the outcomes:

- In Isfahan (i.e., semi-arid climate), a closed liquid absorption cycle solar-thermal system performs best. It resulted in a 27% reduction in operating costs and 40% reduction in gas consumption, saving 8,620 m<sup>3</sup> annually. The initial investment cost can be recovered in approximately 11 years.
- In Kerman (i.e., xx region), the closed-loop liquid absorption cycle in a solar configuration reduces daily fuel consumption from 218 to 142 m<sup>3</sup>, resulting in a 35% annual reduction. Compared to a gas-fired cycle, the solar cycle cuts system operating costs by 26% - saving \$1620 per year - and lowers CO<sub>2</sub> emissions by 26,980 kg annually. The payback period is approximately 8 years.
- In Bushehr (i.e., warm and humid region), a solid desiccant cycle was chosen to control humidity. Hybrid use reduced fuel consumption from 125,907 m<sup>3</sup> to 110,763 m<sup>3</sup> per year and decreased operating costs from \$26,774 to \$24,549 annually. This creates an annual cost savings of \$1,817 and lowers CO<sub>2</sub> emissions by 33,318 kg annually. The payback period is roughly 5.3 years.
- In Tabriz (i.e., mountainous climate), the solar solid desiccant cycle is preferred due to technical, economic, and environmental benefits. It reduces operating costs by \$920 per year and fuel consumption by 54.2 m<sup>3</sup> per day compared to the gas-fired cycle. It also emits approximately 13,851 kg less CO<sub>2</sub> per year and has a payback period of 13.5 years.
- In Ramsar (i.e., moderate humid climate), a solid desiccant cycle is the most suitable system due to the high humidity and impracticality of cooling towers. A solar cycle instead of a gas-fired cycle reduces annual operating costs from \$11,319 to \$10,160, saves 5269 m<sup>3</sup> of natural gas annually, and reduces CO<sub>2</sub> emissions by approximately 14,385 kg. The payback period for this cycle is approximately 10.5 years.
- A 100% increase in solar collector area reduces fuel consumption by 20%. Increasing the slope angle of the collector in summer increases the payback period by 1 year. A 30% increase in the building's floor area improves system efficiency and reduces the payback period by 1 year. Savings are generated by reduced gas consumption, and a 50% reduction in gas rates reduces the payback period. A 10% increase in interest rate reduces the payback period by 1 year. A 50% reduction in initial capital investment cost reduces the payback period to 6-8 years.

**Nomenclature**

A	Area [m <sup>2</sup> ]
a	Collector Panel High [m]
AC	Annual Cost
b	Solar Collector Panel Width [m]
c	Cost Per Unit of Exergy
$\dot{C}$	Exergy Cost Rate
$C_p$	Specific Heat in Constant Pressure [kJ/kgK]
COP	Coefficient of Performance
CV	Annual Costs [USD]
DPV	Discounted Present Value [USD]
E	Primary Energy [kWh]
EX	Exergy [kW]
h	Specific Enthalpy [kJ/kg]
I	Irreversibility [kW]
$i_b$	Beam Irradiation [kWh/ m <sup>2</sup> ]
$i_d$	Diffused irradiation [kWh/m <sup>2</sup> ]
$i_{\text{tilted}}$	Irradiation on Tilted Surface [kWh/m <sup>2</sup> ]
$i_{\text{tot}}$	Total Irradiation [kWh/m <sup>2</sup> ]
Inv	Initial Investment [USD]
ir	Interest Rate
LCC	Life Cycle Cost [USD]
LHV	Lower Heat Value [kJ/kg]
m	Mass [kg]
$\dot{m}$	Mass Flow Rate [kg/s]
n	Day of the Year
NPV	Net Present Value [USD]
P	Pressure [kPa]
PW	Present Worth
Q	Fuel Demand [m <sup>3</sup> ]
$\dot{Q}$	Heat Rate [kW]
R	Universal Gas Constant [3.14 J/mol K]
$R_b$	Beam Irradiation Coefficient
RH	Related Humidity
s	Specific Entropy [kJ /kg K]
SF	Solar Fraction
SPP	Simple Payback Period [Year]
T	Temperature [K]
$T_0$	Dead Sate Temperature [K]
$T_s$	Sun Temperature
V	Volume [m <sup>3</sup> ]
v	Specific Volume [m <sup>3</sup> /kg]
$\dot{W}$	Power Rate [kW]
X	Distance Between Two Rows of Collectors [m]
$\dot{Z}$	Capital Investment

**Greek Letters**

$\alpha_s$	Solar Elevation Angle [deg]
------------	-----------------------------

$\alpha_p$	Portrait Angle [deg]
$\beta$	Solar Collector tilt Angle [deg]
$\gamma_s$	Solar Azimuth Angle [deg]
$\eta$	Energy Efficiency
$\varepsilon$	Exergy Efficiency
$\sigma$	Daily Angle [deg]
$\rho$	Density [kg/ m <sup>3</sup> ]
$\rho_g$	Ground Reflection Factor
$\Phi$	Latitude Angle [deg]
$\Phi_k$	Maintenance Factor
$\omega$	Humidity Ratio
$\acute{\omega}$	Hourly Angle [deg]

**Abbreviations**

AB	Absorption
Abs	Absorber
AD	Adsorption
AUX	Auxiliary
Cond	Condenser
CT	Cooling Tower
Desw	Desiccant Wheel
Evap	Evaporator
EXPV	Expansion valve
F	Fuel
f	Fan
Gen	Generator
HC	Hot Coil
HEX	Heat Exchanger
Hexw	Heat Exchanger Wheel
NG	Natural Gas
P	Pump
Rec	Receiver
SD	Solid Desiccant

**Subscripts**

0	Dead State
1	Scenario 1
2	Scenario 2
AVE	Average
b	Beam
d	Diffuse
g	Ground
in	Inlet
k	Devices
MAX	Maximum
MIN	Minimum
out	Outlet
sys	System
tilted	Titled
tot	Total

## References

- [1] Li, G., et al., *Building integrated solar concentrating systems: A review*. Applied Energy, 2020. 260: p. 114288.
- [2] Asadi, J., et al., *Thermo-economic analysis and multi-objective optimization of absorption cooling system driven by various solar collectors*. Energy Conversion and Management, 2018. 173: p. 715-727.
- [3] Roumpedakis, T.C., et al., *Life cycle analysis of ZEOSOL solar cooling and heating system*. Renewable Energy, 2020. 154: p. 82-98.
- [4] Areeba Rahman, Naeem Abas, Saad Dilshad, Muhammad Shoaib Saleem, *A case study of thermal analysis of a solar assisted absorption air-conditioning system using R-410A for domestic applications*. Case Studies in Thermal Engineering. 2021.
- [5] Abbassi, Y., E. Baniasadi, and H. Ahmadikia, *Comparative performance analysis of different solar desiccant dehumidification systems*. Energy and Buildings, 2017. 150: p. 37-51.
- [6] Ibrahim, N.I., F.A. Al-Sulaiman, and F.N. Ani, *A detailed parametric study of a solar driven double-effect absorption chiller under various solar radiation data*. Journal of Cleaner Production, 2020. 251: p. 119750.
- [7] Maher Shehadi, *Optimizing solar cooling systems*. Case Studies in Thermal Engineering. 2020.
- [8] Shakiba Sharifi, F.N.H., Reza Shirmohammadi, *Comprehensive thermodynamic and operational optimization of a solar-assisted LiBr/water absorption refrigeration system*. Energy Reports, 2020.
- [9] Yue Jinga, Z.L., Liming Liua, Shengzi Lua, Shiliang Lv, *Exergy-economic-optimized design of a solar absorption-subcooled compression hybrid cooling system for use in low-rise buildings*. Energy Conversion and Management, 2018.
- [10] M. Miari Naeimi, M. Eftekhari Yazdi, G.H. Salehi, *Energy, exergy, Exergy-economic and Exergyeconomic analysis and optimization of a solar hybrid CCHP system*. Energy Sources, Part A: Recovery, Utilization, and Environmental Effects, 2019.
- [11] Muhammad Umer Arshad, M.U.G., Atta Ullah, Afşin Güngör, Muhammad Zaman, *Thermodynamic analysis and optimization of double effect absorption refrigeration system using genetic algorithm*. Energy Conversion and Management, 2019.
- [12] Muhammad Salim Ferwati, A.M.A., Gorakshnath Dadabhau Takalkar, *Energy and exergy analysis of parallel flow double effect H<sub>2</sub>O-[mmim][DMP] absorption refrigeration system for solar powered district cooling*. Case Studies in Thermal Engineering, 2021.
- [13] Mohammad Javad Asgari Amin Alaminia, *Exergetic analysis and economic analysis method of a solar cooling system for a residential building application*. Energy system. 2023.
- [14] V. Baiju, A. Asif Sha, C.A. Shajahan, V.G. Chindhu *Energy and exergy based assessment of a two bed solar adsorption cooling system*, International Journal of Refrigeration. 2022.
- [15] M. Mortadi, A. El Fadar, *Performance, economic and environmental assessment of solar cooling systems under various climates*. Energy Conversion and Management. 2022.
- [16] Tareq Salameh, Ammar Alkhalidi, Malek Kamal Hussien Rabaia, *Optimization and life cycle analysis of solar-powered absorption chiller designed for a small house in the United Arab Emirates using evacuated tube technology*, Renewable Energy. 2022.
- [17] Auroshis Rout, Suneet Singh, Taraprasad Mohapatra, Sudhansu S. Sahoo, Chetan Singh Solanki, *Energy, exergy, and economic analysis of an off-grid solar polygeneration system*. Energy Conversion and Management. 2021.
- [18] Sanju Thomas, Sudhansu S. Sahoo, G Ajithkumar, Sheffy Thomas, Auroshis Rout, Swarup K. Mahapatra, *Socio-economic and environmental analysis on solar thermal energy-based polygeneration system for rural livelihoods applications on an Island through interventions in the energy-water-food nexus*. Energy Conversion and Management. 2022.

- [19] Sanju Thomas, A.G. Kumar, Sudhansu S. Sahoo, Shinu M. Varghese, *Energy and exergy analysis of solar thermal energy-based polygeneration processes for applications in rural India*. International Energy Journal. 2018.
- [20] Amin Motevali Emami, Ehsan Baniasadi, Rahil Sadeghi, *Dynamic simulation and exergy-economic assessment of solar thermal refrigeration systems in different climates*. Applied Thermal Engineering. 2023.
- [21] Werner Weiss, M.S.-D., *Solar Heat Worldwide, Global Market Development and Trends in 2019*, , Institute for Sustainable Technologies Gleisdorf, Austria 8200, 2019.
- [22] John A. Duffie, William A. Beckman, *Solar Engineering of Thermal Processes*, Wiley, Fourth Edition.
- [23] Zeyu Li, Liming Liu, Yue Jing, *Exergoeconomic analysis of solar absorption-subcooled compression hybrid cooling system*, Energy Conversion and Management, 2017.
- [24] Somayeh Toghyani, E.B., Ebrahim Afshari, *Thermodynamic analysis and optimization of an integrated Rankine power cycle and nano-fluid based parabolic trough solar collector*. Energy Conversion and Management, 2016.
- [25] Dereje S. Ayou, V.E., *Energy, exergy and Exergyeconomic analysis of an ultra low-grade heatdriven ammonia-water combined absorption power-cooling cycle for district space cooling, sub-zero refrigeration, power and LNG regasification*. Energy Conversion and Management, 2020.
- [26] Jiangjiang Wang, Y.C., Noam Lior, *Exergy-economic analysis method and optimization of a novel photovoltaic/thermal solar-assisted hybrid combined cooling, heating and power system*. Energy Conversion and Management, 2019.
- [27] Giuseppe Bonforte, J.B., Giampaolo Manfrida, Karolina Petela, *Exergyeconomic and Exergyenvironmental Analysis of an Integrated Solar Gas Turbine/Combined Cycle Power Plant*. Energy, 2017.
- [28] Osama Ayadi, S.A.-D., *Comparison of solar thermal and solar electric space heating and cooling systems for buildings in different climatic regions*. Solar Energy, 2019.
- [29] Javad Asadi, P.A., Mohammad Amani, Alibakhsh Kasaeian, Mehdi Bahiraei, *Thermo-economic analysis and multi-objective optimization of absorption cooling system driven by various solar collectors*. Energy Conversion and Management, 2018.
- [30] Whang, A.J.-W., et al., *A review of daylighting system: for prototype systems performance and development*. Energies, 2019. 12(15): p. 2863.
- [31] Wolfram Stephan, Arno Dentel, Thomas Dippel, *Design Handbook for Reversible Heat Pump Systems with and without Heat Recovery*, IEA-ECBCS ANNEX 48, 2011.
- [32] Mugnier, D. and U. Jakob, *Status of solar cooling in the World: markets and available products*. Energy and Environment, 2015. 4(3): p. 229-234.
- [33] Fong K, Chow TT, Lee CK, Lin Z, Chan L. *Comparative study of different solar cooling systems for buildings in subtropical city*. Solar Energy. 2010; 84:227-44.
- [34] Mehdi Sedaghat, Hamid Nazari poor, *A New Approach for Definition of Summer Season in Iran*. Journal of Climate Research. 2018.

## Appendix 1: Technical and economic assumptions

Table A: Technical and thermodynamic parameters

Parameter [unit]	Value	Parameter [unit]	Value	Parameter [unit]	Value
Tabriz Latitude Angle	38	Bushehr Latitude Angle	29	Isfahan Latitude Angle	32.62
AUX Heater Efficiency	0.8	Heat Exchanger Efficiency	0.85	Solar Collectors Efficiency	0.5-0.7
Avg. Density of Natural Gas [kg/m <sup>3</sup> ]	0.8	AVE LHV of Natural Gas [kJ/kg]	48500	Fans & Pumps Efficiency	0.9
AVE Mass Coefficient of NO <sub>x</sub> [kg <sub>NO<sub>x</sub></sub> /kg <sub>fuel</sub> ]	0.00185	AVE Mass Coefficient of CO [kg <sub>CO</sub> /kg <sub>fuel</sub> ]	0.0009	AVE mass Coefficient of CO <sub>2</sub> [kg <sub>CO<sub>2</sub></sub> /kg <sub>fuel</sub> ]	2.75
Aperture Area of Collectors [m <sup>2</sup> ]	150	Ground Reflection Factor	0.25	AVE Inside Room Temperature [°C]	23
Coolant Flow Rate in Absorption Cycle [kg/s]	4	Air Outlet Temperature in Desiccant wheel [°C]	65	Hot Water Pressure in Desiccant Cycle [kPa]	150
Density of Poor flow in Absorption Cycle [kg <sub>LiBr</sub> /kg <sub>solution</sub> ]	0.55	Hot Water Flow Rate in all cycles [kg/s]	2	Cooling Water Flow Rate in Absorption Cycle [kg/s]	4
Cooling Water Pressure in Absorption Cycle [kPa]	200	Coolant Flow Pressure in Absorption Cycle [kPa]	200	Density of Rich flow in Absorption Cycle [kg <sub>LiBr</sub> /kg <sub>solution</sub> ]	0.6
Lower Pressure of Absorption Cycle [kPa]	1	Higher Pressure of Absorption Cycle [kPa]	8	Hot Water Pressure in Absorption Cycle [kPa]	200
Inlet Temperature of Coolant Flow in Evaporator [°C]	15	Hot Water Inlet Temperature in Absorption Cycle [°C]	85	Outlet Temperature of Cooling Tower [°C]	20
Lower Pressure of Adsorption Cycle [kPa]	10	Higher Pressure of Adsorption Cycle [kPa]	70	Quality Factor of Evaporator Outlet Flow [kg <sub>v</sub> /kg]	0.95
Indoor relative humidity	0.5	Indoor pressure [kPa]	102.23	AVE Ambient Pressure [kPa]	101.23
Avg. Wet Bulb Temperature in Bushehr [°C]	30.2	Avg. Ambient Temperature in Isfahan [°C]	38	Selected Day	211
MAX Cooling Load in Kerman [kW]	146	MAX Cooling Load in Ramsar [kW]	189	Selected Hour	14
Sun Surface Temperature [°C]	5800	Ramsar Latitude Angle	36	Kerman Latitude Angle	30
Avg. Ambient Temperature in Bushehr [°C]	42	Avg. Wet Bulb Temperature in Tabriz [°C]	20.5	MAX Cooling Load in Bushehr [kW]	212.4
MAX Cooling Load in Tabriz [kW]	81.3	MAX Cooling Load in Isfahan [kW]	110	Avg. Ambient Temperature in Tabriz [°C]	35
Avg. Wet Bulb Temperature in Isfahan [°C]	22.7	Avg. Ambient Temperature in Kerman [°C]	46	Avg. Ambient Temperature in Ramsar [°C]	36
Avg. Wet Bulb Temperature in Kerman [°C]	24	Avg. Wet Bulb Temperature in Ramsar [°C]	31		

Table B: Assumptions in economic study

Parameter[ <i>unit</i> ]	Value	Parameter[ <i>unit</i> ]	Value	Parameter[ <i>unit</i> ]	Value
Supposed Payback Period for Government Subsidy [Year]	4	Avg. Cost of Electricity Unit [USD/kWh]	0.06	Unit Cost of Natural Gas [USD/m <sup>3</sup> ]	0.12
Interest Rate	5%	Maintenance Factor	0.0125	Discount Rate	2.5%
Exchange Rate EU to USD	1.06	Unit Price of Solar Collectors [USD]	500	30 m <sup>2</sup> Solar Collector Price [USD]	2500
Capital Investment of Adsorption Cycle in Tabriz (Scenario1) [USD]	56350	Capital Investment of Absorption Cycle in Isfahan (Scenario2) [USD]	44696.4	Capital Investment of Absorption Cycle in Isfahan (Scenario1) [USD]	56751
Capital Investment of Solid Desiccant Cycle in Bushehr (Scenario2) [USD]	105219.8	Capital Investment of Solid Desiccant Cycle in Bushehr (Scenario1) [USD]	117012.7	Capital Investment of Adsorption Cycle in Tabriz (Scenario2) [USD]	63974
Capital Investment of Adsorption Cycle in Isfahan (Scenario1) [USD]	96282.9	Capital Investment of Absorption Cycle in Ramsar (Scenario2) [USD]	64985.9	Capital Investment of Absorption Cycle in Ramsar (Scenario1) [USD]	77183.4
Capital Investment of Desiccant Cycle in Isfahan (Scenario2) [USD]	70840.7	Capital Investment of Desiccant Cycle in Isfahan (Scenario1) [USD]	82681.2	Capital Investment of Adsorption Cycle in Isfahan (Scenario2) [USD]	83906.9
Capital Investment of Adsorption Cycle in Kerman (Scenario1) [USD]	117869.5	Capital Investment of Absorption Cycle in Kerman (Scenario2) [USD]	55525.4	Capital Investment of Absorption Cycle in Kerman (Scenario1) [USD]	67841.9
Capital Investment of Desiccant Cycle in Kerman (Scenario2) [USD]	71078.7	Capital Investment of Desiccant Cycle in Kerman (Scenario1) [USD]	82919.2	Capital Investment of Adsorption Cycle in Kerman (Scenario2) [USD]	105672
Capital Investment of Adsorption Cycle in Bushehr (Scenario1) [USD]	152272.4	Capital Investment of Absorption Cycle in Bushehr (Scenario2) [USD]	71649.9	Capital Investment of Absorption Cycle in Bushehr (Scenario1) [USD]	84058.03
Capital Investment of Absorption Cycle in Tabriz (Scenario2) [USD]	35473.9	Capital Investment of Absorption Cycle in Tabriz (Scenario1) [USD]	47849.9	Capital Investment of Adsorption Cycle in Bushehr (Scenario2) [USD]	140074.9
Initial Investment of Adsorption Cycle in Ramsar (Scenario1) [USD]	140788.9	Initial Investment of Desiccant Cycle in Ramsar (Scenario1) [USD]	141895.6	Initial Investment of Adsorption Cycle in Ramsar (Scenario2) [USD]	128948.4
Initial Investment of Desiccant Cycle in Tabriz (Scenario2) [USD]	67270.7	Initial Investment of Desiccant Cycle in Tabriz (Scenario1) [USD]	79111.2	Initial Investment of Desiccant Cycle in Ramsar (Scenario2) [USD]	129757.6

## Appendix 2: Supplementary data

Table. S1: Energy and exergy efficiency values for components in each cooling systems

Component	<i>Absorber</i>	<i>Collector</i>	<i>Condenser</i>	<i>Cooling Tower</i>	<i>Evaporator</i>	<i>Expansion Vavle 1</i>	<i>Expansion Vavle 1</i>	<i>Generator</i>	<i>Aux Heater</i>	<i>Heat Exchanger</i>
<b>Energy Efficiency [%]</b>	85	63	72	47	84	77	91	41	80	85
<b>Exergy Efficiency [%]</b>	36	8	33	81	34	69	88	75	72	75
Component	<i>Adsorber</i>	<i>Collector</i>	<i>Condenser</i>	<i>Cooling Tower</i>	<i>Evaporator</i>	<i>Expansion Vavle</i>	<i>Aux Heater</i>	<i>Reciever</i>	<i>Pump</i>	
<b>Energy Efficiency [%]</b>	88	70	85	60	85	90	80	96	90	
<b>Exergy Efficiency [%]</b>	50.5	13	25	87	27	85	60	73	77	
Component	<i>Collector</i>	<i>Desiccant Wheel</i>	<i>Fan</i>	<i>Aux Heater</i>	<i>Heat Exchanger Wheel</i>	<i>Hot Coil</i>	<i>Pump</i>	<i>Cooler</i>		
<b>Energy Efficiency [%]</b>	70	90	90	80	85	32	90	77		
<b>Exergy Efficiency [%]</b>	12	92	72	73	72	71	81	42		

Table. S2: Comparison between solar cooling systems and common cooling systems

System Type	<i>Annual Cost [\$]</i>	<i>Annual Irreversibility [kWh]</i>	<i>Annual Exergo-Economic Factor</i>	<i>Annual Fuel Demand [m<sup>3</sup>/year]</i>	<i>Annual Primary Energy [kWh]</i>	<i>Annual Exergy Efficiency (<math>\epsilon</math>)</i>	<i>Annual Energy Efficiency (COP)</i>
<b>Solar System Included</b>	3171	270967	0.7074	13447	200193	0.2173	0.8591
<b>Solar System Not Included</b>	4305	281457	0.335	22067	373356	0.157	0.88
<b>Solar System Included</b>	2262	131704	0.74	6497	111467	0.1852	0.6294
<b>Solar System Not Included</b>	3180	138156	0.272	10157	174657	0.136	0.7
<b>Solar System Included</b>	24560	2265000	0.697	110815	1783000	0.1227	0.5782
<b>Solar System Not Included</b>	27700	2259000	0.696	125952	2047896	0.122	0.6

**Declaration of interests**

The authors declare that they have no known competing financial interests or personal relationships that could have appeared to influence the work reported in this paper.

The authors declare the following financial interests/personal relationships which may be considered as potential competing interests:

Journal Pre-proof